REVIEWS



Changing El Niño—Southern Oscillation in a warming climate

Wenju Cai 6 1.2.3 Agus Santoso 3.4.5, Matthew Collins 6, Boris Dewitte 7.8.9, Christina Karamperidou 10, Jong-Seong Kug 11, Matthieu Lengaigne 12, Michael J. McPhaden 13, Malte F. Stuecker 14, Andréa S. Taschetto 4.5, Axel Timmermann 15.16, Lixin Wu 1.2, Sang-Wook Yeh 17, Guojian Wang 1.2.3, Benjamin Ng 3, Fan Jia 18, Yun Yang 19, Jun Ying 20.21, Xiao-Tong Zheng 11.2, Tobias Bayr 22, Josephine R. Brown 23, Antonietta Capotondi 24.25, Kim M. Cobb 26, Bolan Gan 1.2, Tao Geng 1, Yoo-Geun Ham 27, Fei-Fei Jin 10, Hyun-Su Jo 27, Xichen Li 28.29, Xiaopei Lin 12, Shayne McGregor 30, Jae-Heung Park 11, Karl Stein 15.16, Kai Yang 31, Li Zhang 21, and Wenxiu Zhong 21,32

Abstract | Originating in the equatorial Pacific, the El Niño-Southern Oscillation (ENSO) has highly consequential global impacts, motivating the need to understand its responses to anthropogenic warming. In this Review, we synthesize advances in observed and projected changes of multiple aspects of ENSO, including the processes behind such changes. As in previous syntheses, there is an inter-model consensus of an increase in future ENSO rainfall variability. Now, however, it is apparent that models that best capture key ENSO dynamics also tend to project an increase in future ENSO sea surface temperature variability and, thereby, ENSO magnitude under greenhouse warming, as well as an eastward shift and intensification of ENSO-related atmospheric teleconnections — the Pacific-North American and Pacific-South American patterns. Such projected changes are consistent with palaeoclimate evidence of stronger ENSO variability since the 1950s compared with past centuries. The increase in ENSO variability, though underpinned by increased equatorial Pacific upper-ocean stratification, is strongly influenced by internal variability, raising issues about its quantifiability and detectability. Yet, ongoing coordinated community efforts and computational advances are enabling long-simulation, large-ensemble experiments and high-resolution modelling, offering encouraging prospects for alleviating model biases, incorporating fundamental dynamical processes and reducing uncertainties in projections.

The El Niño–Southern Oscillation (ENSO) is the most important climate phenomenon on Earth, driving pronounced interannual changes in the global climate¹⁻³. It describes an alternation between warm phase El Niño and cold phase La Niña events. During El Niño, as in 2015–2016 (REFS^{4,5}), anomalous sea surface temperature (SST) warming in the central and eastern equatorial Pacific weakens the equatorial west-minus-east zonal SST gradient, in turn, weakening the trade winds and intensifying the warm anomaly — a process referred to as Bjerknes feedback⁶. During such events, atmospheric convection (primarily located over the west Pacific) moves eastward. During a La Niña event, anomalously cool SSTs are found in the central and eastern Pacific,

while convection over the western Pacific intensifies and becomes more concentrated.

Such dynamical changes have resulting climatic impacts. For example, during El Niño events, the eastward shift of convection promotes droughts and forest fires in nations bordering the western Pacific, but torrential rains and floods in regions of the eastern equatorial Pacific¹-³,7,8; roughly opposite impacts are observed during La Niña. Indeed, the 1997 El Niño led to huge environmental disruptions, including wildfires in Indonesia that lasted into early 1998, the disappearance of marine life and decimation of the native bird population in the Galápagos Islands³, marine heatwaves¹¹ and bleaching of corals¹¹. During the 1998 La Niña, river floods in China

™e-mail: wenju.cai@csiro.au https://doi.org/10.1038/ s43017-021-00199-z led to the death of thousands and displaced more than 200 million people¹², and over 50% of Bangladesh land area was flooded, leading to severe food shortages and the spread of waterborne diseases, killing several thousand and affecting over 30 million people^{13,14}. ENSO, therefore, affects agriculture, public health, infrastructure, transportation, water security, ecosystems and biodiversity^{1–3,15}. There is, thus, clear societal need to understand observed and projected ENSO responses to greenhouse warming, particularly in light of growing anthropogenic emissions of greenhouse gases^{16,17}, so as

Author addresses

¹Frontier Science Centre for Deep Ocean Multispheres and Earth System and Physical Oceanography Laboratory, Ocean University of China, Qingdao, China.

 $^2\mathrm{Qingdao}$ National Laboratory for Marine Science and Technology (QNLM), Qingdao, China.

³Centre for Southern Hemisphere Oceans Research (CSHOR), CSIRO Oceans and Atmosphere, Hobart, TAS, Australia.

⁴Climate Change Research Centre (CCRC), University of New South Wales, Sydney, NSW, Australia.

⁵ARC Centre of Excellence for Climate Extremes, University of New South Wales, Sydney, NSW, Australia.

⁶College of Engineering, Mathematics and Physical Sciences, University of Exeter, Exeter, UK.

⁷Centro de Estudios Avanzados en Zonas Áridas (CEAZA), La Serena, Chile.

⁸Departamento de Biología Marina, Facultad de Ciencias del Mar, Universidad Católica del Norte, Coquimbo, Chile.

⁹Millennium Nucleus for Ecology and Sustainable Management of Oceanic Islands (ESMOI), Coquimbo, Chile.

¹ºDepartment of Atmospheric Sciences, University of Hawai'i at Mānoa, Honolulu, HI, USA.
¹¹Division of Environmental Science & Engineering, Pohang University of Science and Technology (POSTECH), Pohang, South Korea.

¹²MARBEC, Université Montpellier, CNRS, Ifremer, IRD, Sète, France.

¹³NOAA Pacific Marine Environmental Laboratory (PMEL), Seattle, WA, USA.

¹⁴Department of Oceanography and International Pacific Research Center, School of Ocean and Earth Science and Technology, University of Hawaiʻi at Mānoa, Honolulu, HI, USA.

¹⁵Center for Climate Physics, Institute for Basic Science (IBS), Busan, South Korea.
¹⁶Pusan National University, Busan, South Korea.

 $^{\rm 17}{\rm Department}$ of Marine Sciences and Convergent Technology, Hanyang University, Ansan, South Korea.

¹⁸CAS Key Laboratory of Ocean Circulation and Waves, Institute of Oceanology/Center for Ocean Mega-Science, Chinese Academy of Sciences, Qingdao, China.

 $^{\rm 19}$ College of Global Change and Earth System Science, Beijing Normal University, Beijing, China.

²⁰State Key Laboratory of Satellite Ocean Environment Dynamics, Second Institute of Oceanography, Ministry of Natural Resources, Hangzhou, China.

²¹Southern Marine Science and Engineering Guangdong Laboratory (Zhuhai), Zhuhai, China.
²²GEOMAR Helmholtz Centre for Ocean Research, Kiel, Germany.

²³School of Geography, Earth and Atmosphere Sciences, University of Melbourne, Parkville, VIC, Australia.

²⁴NOAA Physical Sciences Laboratory, Boulder, CO, USA.

 $^{25}\textsc{Cooperative}$ Institute for Research in Environmental Sciences, University of Colorado Boulder, Boulder, CO, USA.

 $^{\rm 26} School$ of Earth and Atmospheric Sciences, Georgia Institute of Technology, Atlanta, GA, USA.

²⁷Department of Oceanography, Chonnam National University, Gwangju, South Korea.

²⁸Institute of Atmospheric Physics, Chinese Academy of Sciences, Beijing, China.

²⁹University of Chinese Academy of Sciences, Beijing, China.

³⁰School of Earth, Atmosphere & Environment, Monash University, Clayton, VIC, Australia.

³¹State Key Laboratory of Numerical Modeling for Atmospheric Sciences and Geophysical Fluid Dynamics, Institute of Atmospheric Physics, Chinese Academy of Sciences, Beijing, China.

³²School of Atmospheric Sciences and Guangdong Province Key Laboratory for Climate Change and Natural Disaster Studies, Sun Yat-sen University, Guangzhou, China.

to inform adaptation options and enhance mitigation of adverse effects.

Potential future changes in ENSO and the underlying dynamics have, therefore, been well assessed, with ever-evolving fundamental insights (FIG. 1). For example, in a framework of ocean–atmosphere instability^{18–20}, a mean state change with weakened trade winds and a reduced west-minus-east zonal SST gradient, as projected by most climate models^{16,17}, implies that ENSO would become more unstable and favour greater amplitude events under warming²⁰. However, climate models have shown no consensus on ENSO SST variability change in conventionally defined regions of the central-eastern equatorial Pacific^{21–24}.

Instead, models that more realistically simulate characteristics of extreme ENSO events tend to project systematic changes 17. These changes include an increased frequency of El Niño events with extreme rainfall in the eastern equatorial Pacific²⁵⁻²⁸, more frequent extreme equatorward swings of large-scale convergence zones^{29,30}, a higher frequency of El Niño events featuring eastward propagating SST anomalies31 and a higher frequency of extreme La Niña events³². Such projected changes are consistent with proxy records of ENSO variability, which suggest that twentieth century ENSO activity is stronger than observed during previous centuries^{33–35}. Indeed, although uncertainty remains, an inter-model consensus on increased ENSO SST variability is emerging³⁶. Advances also continue in understanding the processes controlling mean state changes³⁷⁻⁴⁰, ENSO's interactions with other ocean basins⁴¹ and the role of internal variability42-45.

In this Review, we summarize ENSO projections under anthropogenic warming, specifically building on advances since the previous synthesis in 2015 (REF. 17). We begin by describing ENSO event diversity and asymmetry, changing ENSO in observations and proxy data, and mean state impacts on ENSO feedbacks. We follow with a discussion of the factors that contribute to the observed and projected mean state changes. We continue by outlining the projected ENSO SST variability change and associated mechanisms, focusing on mean state changes, internal variability and inter-basin interactions. We then synthesize insight from palaeo-proxy records of ENSO sensitivity to external forcing. The Review ends with identification of uncertainties and prospects for improved quantification, detection and high-resolution modelling of ENSO SST variability change.

ENSO in observations

Observations of the ocean–atmosphere system over past decades are essential for describing, understanding and modelling ENSO in a warming climate. These observations have shown that no two ENSO events are the same — governed, in part, by differing relative importance of various feedback processes — and that ENSO has been changing.

ENSO event diversity and asymmetry

An important advance in ENSO understanding is that events are diverse in terms of the magnitude, duration, and location of SST anomalies^{5,8,46–51}. Strong El Niño

Key points

- Under anthropogenic warming, the majority of climate models project faster background warming in the eastern equatorial Pacific compared with the west. The observed equatorial Pacific surface warming pattern since 1980, though opposite to the projected faster warming in the equatorial eastern Pacific, is within the inter-model range in terms of sea surface temperature (SST) gradients and is subject to influence from internal variability.
- El Niño-Southern Oscillation (ENSO) rainfall responses in the equatorial Pacific are projected to intensify and shift eastward, leading to an eastward intensification of extratropical teleconnections.
- ENSO SST variability and extreme ENSO events are projected to increase under greenhouse warming, with a stronger inter-model consensus in CMIP6 compared with CMIP5. However, the time of emergence for ENSO SST variability is later than that for ENSO rainfall variability, opposite to that for mean SST versus mean rainfall.
- Future ENSO change is likely influenced by past variability, such that quantification
 of future ENSO in the only realization of the real world is challenging.
- Although there is no definitive relationship of ENSO variability with the mean zonal SST gradient or seasonal cycle, palaeoclimate records suggest a causal connection between vertical temperature stratification and ENSO strength, and a greater ENSO strength since the 1950s than in past centuries, supporting an emerging increase in ENSO variability under greenhouse warming.

events, for example, tend to have SST anomaly centres that peak in the eastern Pacific (EP). The magnitudes of these anomalies are typically larger than the La Niña equivalents but persist for a shorter time. In contrast, strong La Niña and moderate El Niño events tend to peak in the central Pacific (CP) region, with the former also lasting for multiple years (FIG. 2).

The fundamental dynamics of this ENSO diversity and asymmetry relates to a nonlinear Bjerknes feedback^{52–54} in the eastern equatorial Pacific; only after warming surpasses a threshold and rare local deep atmospheric convection is triggered, do zonal winds start to respond to additional warming. The nonlinear zonal wind response leads to further warming, resulting in an extreme EP El Niño. This nonlinear process is distinctively weaker in the CP, where background ocean SST is high and atmospheric convection occurs frequently^{50–52}.

Assessments of observed ENSO evolution and associated feedbacks, therefore, need to consider this diversity. To do so, indices encompassing the different

regions are required. EP ENSO and CP ENSO events can be approximated by spatially fixed indices of SST anomalies, including Niño3 (averaged SST anomaly over 5°S-5°N, 150°W-90°W) for the EP, Niño4 (5°S-5°N, 160°E-150°W) for the CP and Niño3.4 (5°S-5°N, 170°W-120°W) as a combination of the two. Mathematically, the conflicting dynamics between the EP and the CP can be further reflected by a nonlinear relationship between the leading two modes of empirical orthogonal functions of tropical Pacific SST anomalies⁵³. The anomaly pattern associated with the first principal component (PC1) time series features warming in the central-to-eastern equatorial Pacific and the pattern associated with PC2 features warming in the central but cooling in the western and eastern equatorial Pacific. The linear combination of these empirical orthogonal functions represents EP and CP ENSO events, referred to as E-index defined as $(PC1 - PC2)/\sqrt{2}$ and C-index defined as $(PC1 + PC2)/\sqrt{2}$, respectively^{36,52-54}. For observations, time series of Niño3 and Niño4 qualitatively represent the E-index and the C-index (FIG. 2a,b).

ENSO feedbacks and mean state

In addition to event diversity, the background climate state of the equatorial Pacific influences ENSO responses to greenhouse warming via impacts on feedback mechanisms^{1,18–20}. Several ocean—atmosphere feedbacks have been identified as responsible for ENSO SST anomaly growth, some positive and some negative. During an El Niño, mean upwelling of cold subsurface water in the eastern equatorial Pacific and mean horizontal advection act to strengthen the climatological horizontal and vertical SST gradients, and, thus, dampen an initial warm SST anomaly. In addition, the warm SST anomaly promotes deep atmospheric convection, increasing tropical cloud cover and, consequently, reducing surface radiative and latent and sensible heat fluxes into the ocean — a process referred to as thermal damping.

Other positive feedbacks, however, act to amplify or reinforce the initial SST anomalies and west-minus-east SST gradient via weakened equatorial trade winds^{16,55-57}: the Ekman feedback, in which the weakened trade winds reduce upwelling of mean cold subsurface water in the

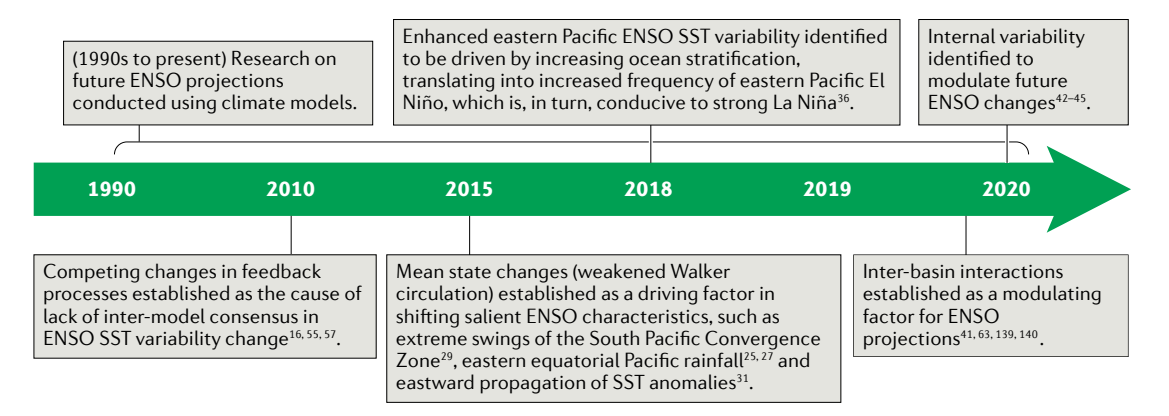


Fig. 1 | Key developments in understanding El Niño–Southern Oscillation response to greenhouse forcing. A timeline illustrating the evolution of thinking regarding El Niño–Southern Oscillation (ENSO) changes in a warming climate. Each development is marked at an approximate time, starting in the 1990s, when climate models were first used to study ENSO future projections 23,24 . SST, sea surface temperature.

eastern equatorial Pacific; the thermocline feedback, whereby the weakened trade winds lead to a flattened thermocline with anomalously warm subsurface water that is advected by mean upwelling to the surface; and the zonal advective feedback, in which the weakened trade winds reduce the mean westward oceanic transport of cold waters from the EP. The relative importance of the feedback processes differs across events; during a CP El Niño, for instance, the zonal advective feedback tends to be more important than the thermocline feedback. Nonetheless, the three positive feedbacks increase with the upper-ocean stratification of the equatorial Pacific^{36,58-61}.

Observed ENSO changes

With understanding of ENSO diversity, it is possible to track observed changes in ENSO characteristics, providing important context to evaluate any future or projected changes. Since the late 1950s, CP and EP ENSO variability has increased 62-64. Indeed, comparing the standard deviation of SST anomalies pre-1960 and post-1960 illustrates an approximately 20% increase in both EP and CP variability (FIG. 2a,b), characterized by more frequent extreme El Niño and La Niña events, respectively. EP and CP ENSO events also now tend to originate and evolve from the western Pacific, rather than the central and eastern Pacific that typified events prior to the 1970s 65.66. Data uncertainty prior to 1950 owing to sparse observations and sampling errors 67, however, challenges interpretation of these changes.

Yet, multiple palaeo-ENSO proxies also provide observational evidence for contemporary ENSO changes. These include a ~25% intensification of ENSO variability during the late twentieth century relative to the pre-industrial period or before $^{33-35,68-71}$, and enhanced CP 69,72 and EP 33 ENSO variability relative to the pre-industrial era. While these results imply that anthropogenic greenhouse forcing might have already contributed to an increase in ENSO variability, because these proxy records reflect ENSO-related temperature and rainfall variability, the extent to which SST variability has increased is unclear.

Changes in the mean state

Given the impact on ENSO feedback mechanisms, changes in the mean state of the equatorial Pacific have strong bearing on ENSO responses to greenhouse warming. Based on ocean-atmosphere reanalyses⁷³⁻⁷⁸, observed mean state changes since the 1980s feature a substantial strengthening of the Walker circulation, the west-minus-east SST gradient and equatorial easterly winds (FIG. 3a). However, the multi-model average changes over the same period are small (FIG. 3b) and the projected future changes generally opposite to those observed: a weakening of the Walker circulation, a reduction of the equatorial west-minus-east SST gradient and an enhanced equatorial warming compared with off-equatorial regions^{16,17} (FIG. 3a-c). Although changes in the west-minus-east SST gradient differ, several models do, in fact, simulate an increasing trend

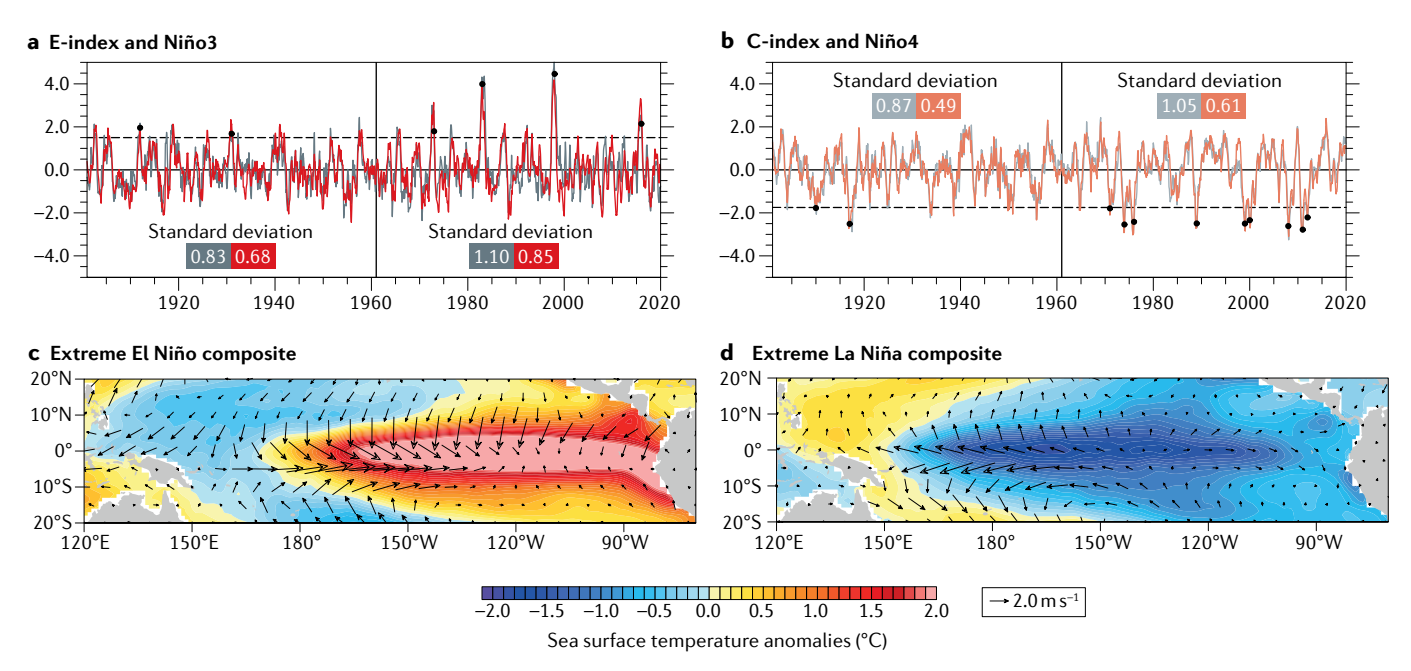


Fig. 2 | Observed El Niño–Southern Oscillation indices and their spatial representation. $\bf a$ | Niño3 (red) and E-index (black) time series from 1901–2020. Values in boxes indicate the standard deviations of the indices calculated over 1901–1960 and 1961–2020. $\bf b$ | As in panel $\bf a$, but for Niño4 (orange) and C-index (grey). $\bf c$ | Composite sea surface temperature and surface wind anomalies for extreme El Niño events; those where the December-January-February mean E-index > 1.5 standard deviations (black dots in panel $\bf a$). $\bf d$ | As in panel $\bf c$, but for extreme La Niña events; those where the December-January-February mean C-index < $\bf -1.75$ standard

deviations (black dots in panel **b**). All panels are based on the average across three products $^{73-75}$. E-index and C-index are calculated by an empirical orthogonal function analysis on tropical Pacific sea surface temperature anomalies 53 , which gives two leading principal component (PC1 and PC2) time series. E-index is defined as (PC1 – PC2)/ $\sqrt{2}$ and C-index is defined as (PC1+PC2)/ $\sqrt{2}$. The increased variability of the Niño3 or E-index in the post-1960 period is characterized by an increased frequency of extreme El Niño events, and increased variability in the Niño4 or C-index by an increased frequency of extreme La Niña.

over 1980–2019 (FIG. 3e) before the long-term reductions emerge in the projections (FIG. 3f). Models also continue to show a persistent cold tongue bias, being too cold and located too far west, as shown in a comparison between a multi-model mean and the observed equatorial mean state (FIG. 3d), with implications for projections^{79,80}, the potential impact of which will be discussed later.

Forcing contemporary mean state changes

Observed changes in the mean state — in particular, the enhanced west-minus-east SST gradient — result from several offsetting or compensating processes, including atmospheric damping differential between the west and the east, an oceanic thermostat mechanism in the east, internal variability on multidecadal scales and inter-basin interactions. These different processes contribute to the observed changes, but not all processes produce the same sign of trends.

West-east damping differential. Higher mean SSTs in the western Pacific result in enhanced thermal damping due to evaporation^{81–83} and greater net negative cloud-radiation feedback (whereby clouds reduce incoming shortwave radiation)⁸⁴ in the west compared with the east. These two processes are unfavourable for SST warming in the western Pacific relative to the east, reducing the equatorial west-minus-east zonal SST gradient⁸³. This reduction, in turn, weakens equatorial easterly winds through Bjerknes feedback, enhancing equatorial warming in the east^{81,82}, further reducing the zonal SST gradient.

Ocean thermostat. Assuming that the ocean is in quasi-equilibrium with greenhouse gas forcing, changes in atmospheric processes must be compensated by changes in oceanic processes. For example, ocean upwelling in the eastern equatorial Pacific can facilitate divergence of some of the heat away from the EP cold tongue region — an ocean thermostat mechanism⁸⁵. This ocean thermostat favours less warming in the EP compared with the western Pacific, which is also amplified by Bjerknes feedback, contributing to an enhanced zonal SST gradient.

Internal variability. Multidecadal internal variability might also contribute to the observed enhancement of the zonal SST gradient since 1980. However, limitations of in situ observations and reanalyses hinder unambiguous attribution of equatorial Pacific trends to natural or anthropogenic causes 40,86. For instance, satellite-observed changes indicate a smaller strengthening of the Walker circulation than implied by reanalyses40. While the satellite trend is still opposite to the simulated changes averaged over large ensembles of model simulations, some ensemble members are also able to reproduce the observed strengthening of the Walker circulation⁴⁰ and the equatorial zonal SST gradients⁸⁶ (FIG. 3e), despite an overall underestimation of internal decadal variability87. Thus, internal multidecadal variability could be offsetting greenhouse-warming-induced changes and, therefore, lead to the observed trend^{40,86,88}, which is potentially transient in nature86.

Inter-basin interactions. Interactions with the tropical Indian and Atlantic oceans on multidecadal timescales are also important in forcing the observed intensification of zonal SST gradient⁴¹ (FIG. 3a). In particular, faster warming in the tropical Indian and/or Atlantic oceans since 1980 has contributed to anomalous atmospheric sinking in the central tropical Pacific^{89–93}. This sinking is conducive to enhanced equatorial easterly surface winds and, hence, to a cooling in the EP⁹⁰.

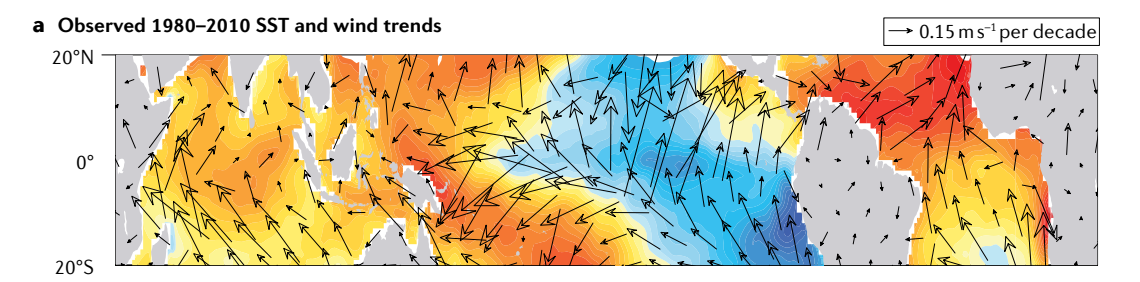
Factors affecting mean state projections

For the projected long-term mean state changes, the competing processes between the atmospheric damping differential and the oceanic thermostat mechanism also operate, whereas multidecadal internal variability has a diminishing role. State-of-the-art climate models also underestimate inter-basin interactions^{37,41,94-96}, which might contribute to the long-term faster warming in the equatorial EP than would otherwise be the case⁴¹. Additional factors that influence future mean state changes include the impact of off-equatorial Pacific Ocean warming, ENSO rectification and cold tongue bias in climate models. The relative importance of each of these factors is unclear and likely model-dependent.

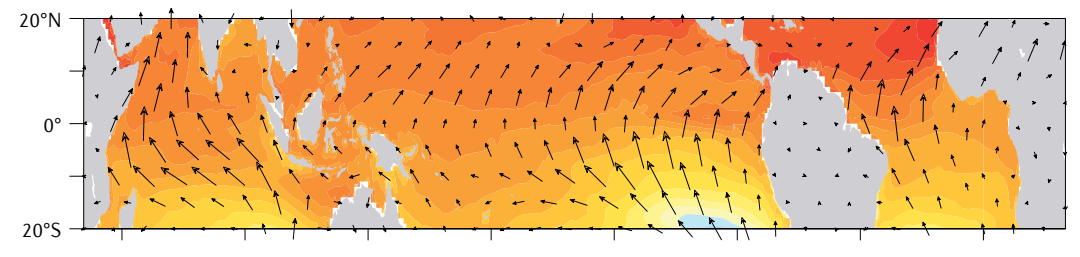
Off-equatorial Pacific warming. Equatorial Pacific mean state changes involve processes outside the equator. For instance, equatorial warming can partly be forced by oceanic subduction of anomalous off-equatorial warming advected towards the equatorial upwelling region or a weakening of the Hadley circulation and wind-driven oceanic subtropical overturning cells^{97,98}. Owing to the multidecadal timescales involved in such forcing, models suggest an initial strengthening of the zonal SST gradient from the oceanic thermostat mechanism, followed decades later by a gradient weakening through oceanic subduction of anomalous off-equatorial warming^{97–99}. Indeed, a model that simulates historical strengthening of the zonal SST gradient commonly exhibits a reversed future trend⁸⁶.

ENSO rectification. While mean state changes can modify the balance of ENSO feedbacks and variability^{36,80,100}, ENSO variability change can also rectify the mean state, altering the warming pattern in the tropical Pacific via nonlinear oceanic temperature advection^{101,102}. For example, if extreme El Niño events become less frequent relative to La Niña events, a La Niña-like mean state warming can emerge¹⁰¹. In models with realistic nonlinear dynamical heating or Bjerknes feedback, an increase in ENSO variability contributes to the emergence of an El Niño-like warming pattern^{36,102}.

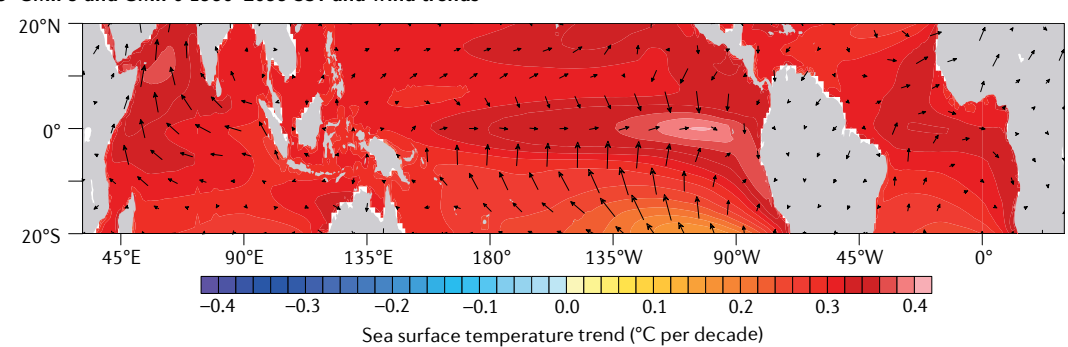
Cold tongue bias. Model biases within the tropical Pacific are suggested to have contributed to a fast warming in the east in most climate models^{37–39}. For example, the common too-cold and too-west cold tongue (FIG. 3d) might produce excessive SST sensitivity to radiative warming in the cold tongue region, resulting in the erroneous warming and weakening in west-minus-east SST gradient³⁹. Conversely, the cold tongue bias can also lead to an overestimated ocean thermostat mechanism under greenhouse warming, spuriously weakening shortwave radiation reduction



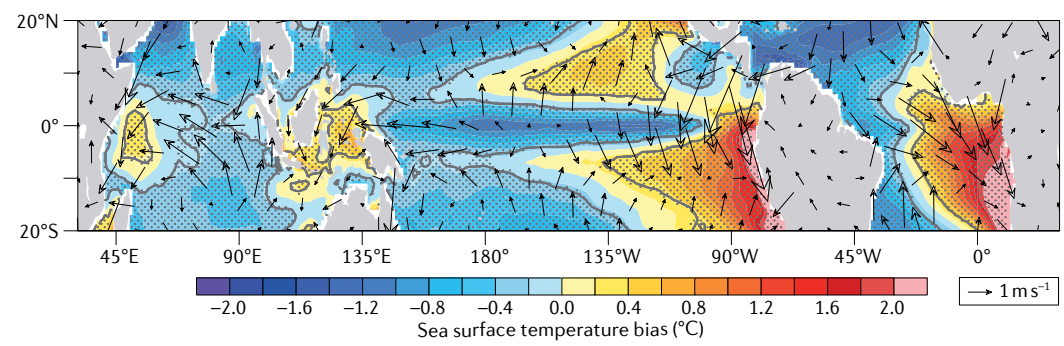
b CMIP5 and CMIP6 1980–2010 SST and wind trends



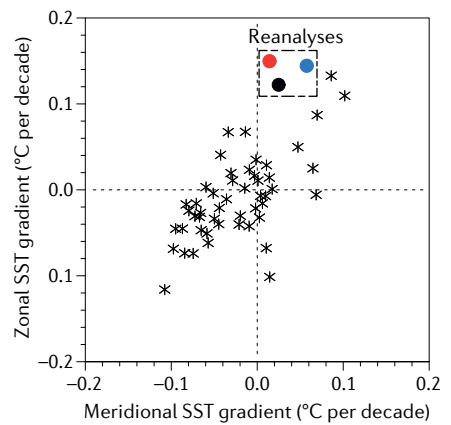
c CMIP5 and CMIP6 1980-2099 SST and wind trends



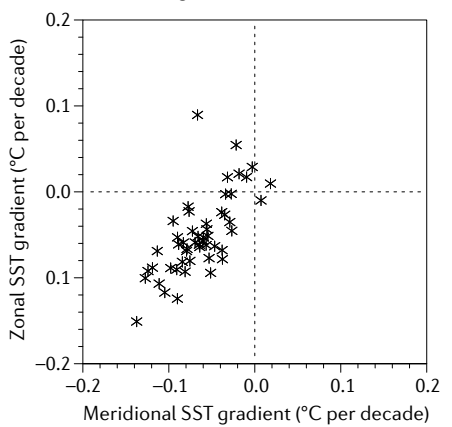
d CMIP5 and CMIP6 1980-2010 SST and wind bias







f 2020-2099 SST gradient trend



▼ Fig. 3 | Observed and simulated tropical Pacific mean state and change. a | Observed sea surface temperate (SST)⁷³⁻⁷⁵ and surface wind⁷⁶⁻⁷⁸ trends calculated over 1980–2010. **b** Average SST trends from 28 CMIP5 and 23 CMIP6 models calculated over 1980–2010; models are forced by historical forcing and the Representative Concentration Pathway 8.5 (RCP8.5) emission scenario or the Shared Socioeconomic Pathway 5-8.5 (SSP5-8.5). c | Average SST trends from 28 CMIP5 and 23 CMIP6 models calculated over 1980–2099. d | CMIP5 and CMIP6 climatological mean SST and surface wind bias relative to the observations for the 1980-2010 period. Stippling and black contours indicate the 90% and 95% confidence levels, respectively, as determined from a two-tailed t-test. e Linear trends in December-January-February zonal and meridional SST gradients over 1980-2019 for the 51 CMIP5 and CMIP6 models (stars) and three reanalysis datasets^{73–75} (circles). **f** | As in panel **e**, but for 2020–2099. In both panels **e** and **f**, zonal SST gradient is defined following REF.86 except sign-reversed; that is, the eastern Pacific $(5^{\circ}S-5^{\circ}N, 180^{\circ}E-80^{\circ}W)$ area average SST is subtracted from the western Pacific $(5^{\circ}S-5^{\circ}N, 180^{\circ}E-80^{\circ}W)$ 110°E-180°E) area average SST. The eastern Pacific meridional SST gradient is defined as the area average off-equatorial northern SST (5°N-10°N, 90°W-150°W) and the southern SST (5°S-10°S, 150°W-90°W) minus the equatorial SST (2.5°S-2.5°N, 90°W-150°W). Approximately 50% of models exhibit the same 1980-2019 west-minus-east SST gradient trend as observations, but most project opposite long-term trends.

in response to surface warming in the central-to-western Pacific¹⁰³. Correction of this bias would, thus, favour a faster EP warming than in the west¹⁰⁰. Despite the disparity between the observed and projected changes, they might not be unidirectional but time-varying⁹⁹. For example, the change in mean west-minus-east SST gradient could initially be dominated by the oceanic thermostat but subsequently by other processes, leading to opposite trends in the late twenty-first century^{97–99}.

Several offsetting processes, thus, contribute to the observed change in the mean west-minus-east SST gradient. The relative contribution of these processes changes from the observed to the projected climate, with the latter influenced by the cold tongue bias, weak inter-basin interactions and rectification of changing ENSO variability, as will now be discussed.

Projected ENSO changes

Model projections of ENSO SST change have generally been based on conventional ENSO SST indices evaluated at fixed anomaly centres^{16,17,42,104}, such as Niño3, without considering ENSO diversity. Projected changes in SST variability at these fixed centres show no inter-model consensus. This lack of inter-model consensus is related, in part, to competing changes between the main linear positive and negative ENSO feedbacks, despite robust change being present in individual feedback terms^{16,55,57,105,106} (FIG. 1).

However, robust projections have now emerged for key characteristics that underpin ENSO extremes^{25,27,31,32,80,107–110} (FIG. 1). For example, the frequency of El Niño events with extreme rainfall impacts is projected to double from about one event per 20 years from 1890–1990 to one event per 10 years over 1990–2090 (REF.²⁷). Such increasing frequency is also seen in CMIP6 models^{26,110} and continues for as long as a century after global mean temperature stabilizes at 1.5–2.0 °C warming relative to the pre-industrial level^{28,109}.

Increased ENSO SST variability

The locations of ENSO SST anomaly centres can differ by as much as 30° longitude between observations and models, and across different models³⁶. Assessment of ENSO SST variability change should, therefore, consider CP and EP ENSO anomaly centres simulated in individual models. Indeed, apparent increases in model agreement regarding ENSO projections can partly be linked to correcting for model-specific anomaly centres³⁶.

For example, in CMIP5 models that reasonably simulate the distinction between EP and CP events, a 15% increase in EP ENSO variance is projected between 1900-2000 and 2000-2100 under a business-as-usual emission scenario for 88% of models³⁶. CP ENSO variance is also anticipated to increase, but only in 59% of models³⁶. CMIP6 models also support these findings¹¹⁰. For instance, 100% of 23 CMIP6 models indicate enhanced EP ENSO variance in the future (FIG. 4a), while 65% generate an increase in CP ENSO variance (FIG. 4b). Even without model selection, the majority of CMIP6 models generate an increase in Niño3 and Niño4 SST variability, with 28 and 27 out of 34 models, respectively, producing an increase of about 10-15% when comparing variability over the twentieth and twenty-first centuries. This stronger inter-model agreement might be related to modest improvements in simulated ENSO patterns and event diversity, and a slight reduction in the Pacific mean state biases111,112.

The enhanced variability in EP and CP ENSO is associated with increased occurrence of extreme EP El Niño and extreme La Niña events³⁶ (FIG. 4c,d). Indeed, extreme El Niño and La Niña events are both projected to increase from 5.6 events per century in the present day to 8.9 and 8.3 events per century in the future climate, respectively. In particular, dramatic swings from an extreme EP El Niño to an extreme La Niña the next year due to El Niño-induced equatorial subsurface heat discharge, as seen in 1997–1998, increase from 1.1 events per century in the present day to 2.8 events per century in the future climate (FIG. 4c,d).

Eastward teleconnection intensification

In the presence of faster warming in the eastern equatorial Pacific Ocean than in the surrounding regions, even weak El Niño events are able to induce strong convection^{17,27,58,108}, leading to subsequent impacts via atmospheric teleconnections. Changes in the amplitude and location of ENSO-related SST variability have the potential to further modify such teleconnections.

As a result of projected faster warming in the eastern equatorial Pacific, mean convection centres shift eastward¹¹³⁻¹²³ and rainfall responses strengthen²⁵⁻²⁷ during both CP and EP ENSO events (FIG. 5). Despite uncertainties in early generations of CMIP models^{122,123}, ENSO-induced Rossby wave trains — such as the Pacific–North American and Pacific–South American teleconnection patterns — are, thus, also projected to shift eastward^{7,113-123}. The high-pressure centre near the Amundsen Sea during peak EP ENSO, for example, shifts by more than 30° longitude (FIG. 5c). The large deepening or shallowing of the North Pacific trough in the Pacific–North American teleconnection is further likely to attain a stronger sensitivity to CP SST anomalies than to EP SST anomalies under greenhouse warming¹¹⁶ (FIG. 5c,d).

These projected changes have important climatic implications for affected regions. For example, as the

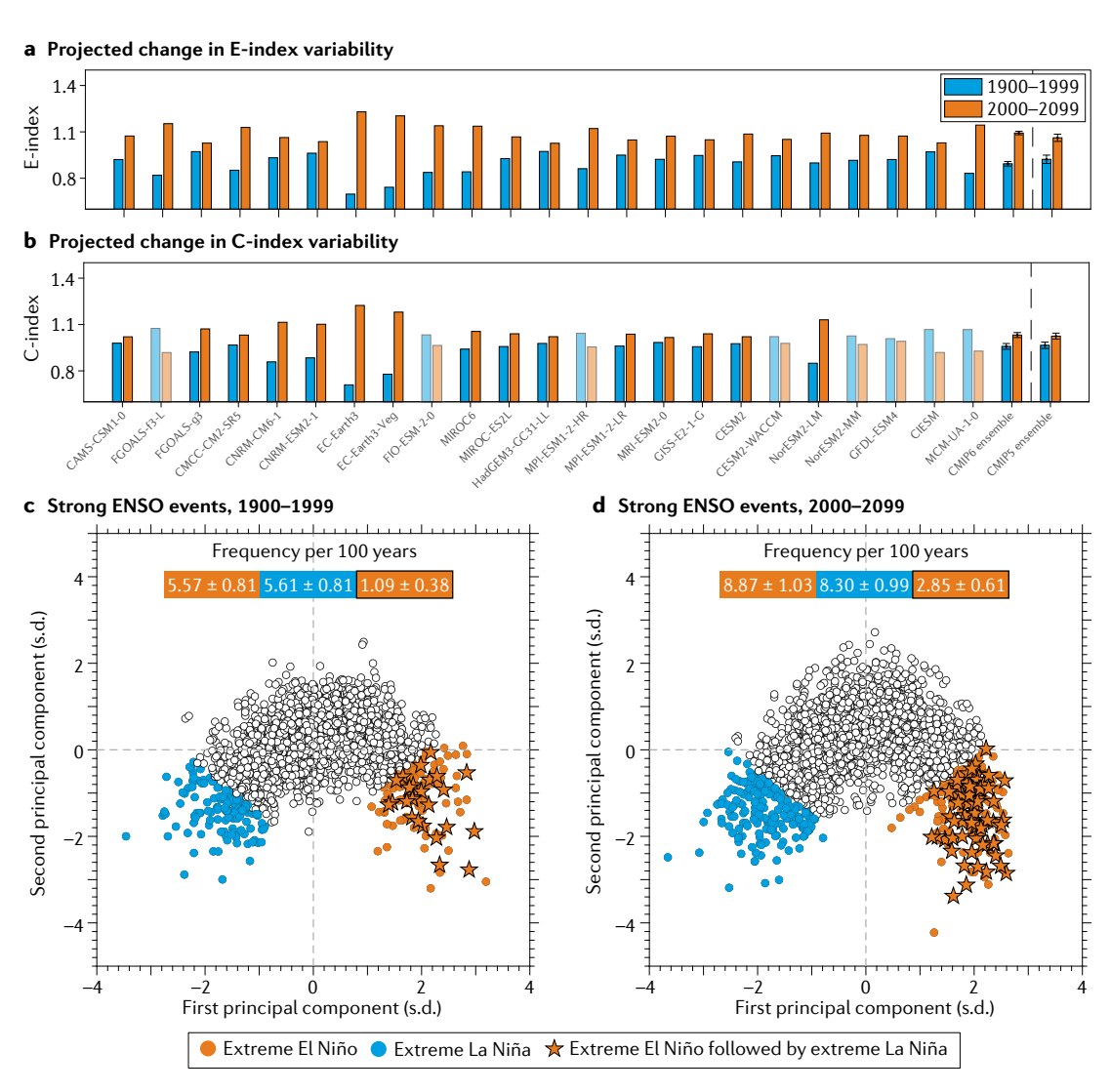


Fig. 4 | **Projected increase in El Niño–Southern Oscillation sea surface temperature variability in CMIP6 models. a** | December-January-February E-index standard deviation over the present (1900–1999; blue) and future (2000–2099; orange) periods for 23 CMIP6 models, and the ensemble mean for CMIP6 and CMIP5 models. Error bars for the multi-model means indicate one standard deviation value of 10,000 realizations in a bootstrap test. **b** | As in panel **a**, but for the C-index. Transparent bars represent those models that simulate a variance reduction. **c** | The relationship between the first and second principal component time series of empirical orthogonal function analysis of sea surface temperature (SST) anomalies 1900–1999 for the identification of extreme El Niño–Southern Oscillation (ENSO) events. Orange dots indicate extreme El Niño events (E-index > 1.5 standard deviations), blue dots extreme La Niña events (C-index <= -1.75 standard deviations) and orange stars with black outlines extreme El Niño events with an extreme La Niña event the following year. Numbers indicate the average frequency of event type per 100 years with 90% confidence interval based on a Poisson distribution. **d** | As in panel **c**, but for 2000–2099. A stronger inter-model consensus on increased ENSO SST variability emerges in CMIP6 than CMIP5 models. Only those models that simulate ENSO nonlinearity at least 50% of the observed (as indicated by the nonlinear relationship between the first and second principal components of SST variability in the tropical Pacific³⁶) are selected. Models are forced by historical forcing up to 2014 and, thereafter, the Shared Socioeconomic Pathway 5-8.5 (SSP5-8.5).

ENSO-induced Pacific–North American pattern shifts eastward, El Niño-induced rainfall anomalies are expected to intensify on the west coast of North America and El Niño-induced surface warming to expand eastward to occupy all of northern North America¹¹³. As a consequence, many regions affected by ENSO in the present climate are likely to experience more intense ENSO-driven rainfall variability in the future¹²⁴.

In addition, owing to increased mean state moisture and increased ENSO variability under greenhouse

warming, the asymmetric atmospheric response between El Niño and La Niña are expected to increase ^{115,120}. As a result, over many land areas, there will be a robust increase in the spatial extent of ENSO teleconnections during austral summer in both temperature and precipitation ¹²⁵, leading to an increased impact in El Niño-induced droughts ^{126,127}. Furthermore, the projected increase in El Niño amplitude provides more favourable large-scale conditions for tropical cyclone formation in the tropical Pacific ^{128,129}, such that island states, such as

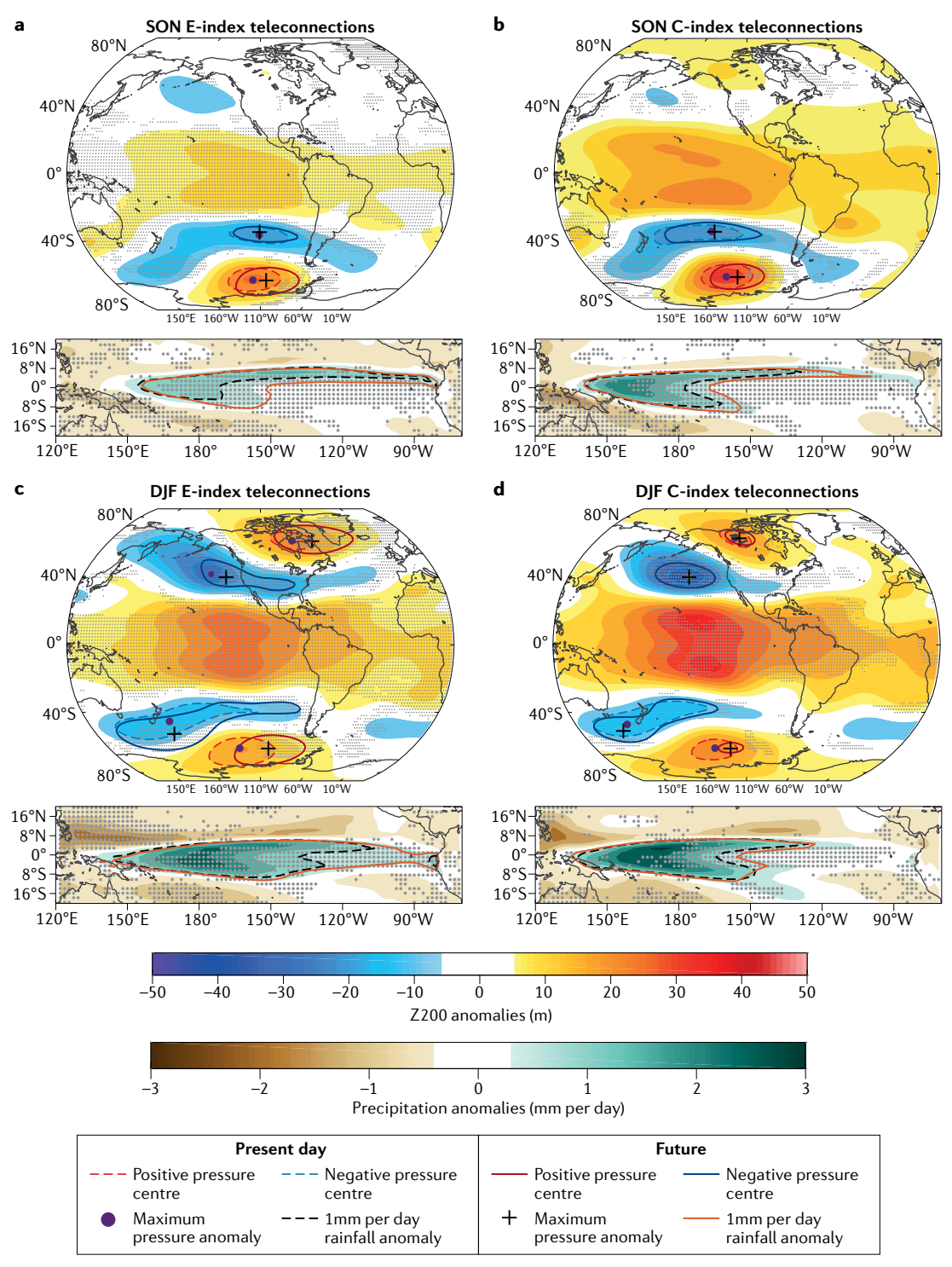


Fig. 5 | Changing El Niño–Southern Oscillation teleconnections under greenhouse warming. a | Regressions of CMIP6 quadratically detrended September-October-November (SON) 200 hPa geopotential height (upper panel) and rainfall anomalies (lower panel) onto the normalized E-index for the present (1900–1999; shaded) and future (2000–2099) periods. Purple dots and dashed coloured contours in the upper panels mark the centre of the El Niño–Southern Oscillation (ENSO)-induced teleconnection (incorporating the Pacific–South American and Pacific–North American teleconnections) for the present period; black crosses and solid contours mark the centre of pressure anomalies for the future period. Dashed black and solid orange contours in the precipitation panel mark the 1 mm per day anomaly for the present and future periods, respectively. b | As in panel a, but regressions of SON anomalies onto the C-index. c | As in panel a, but for December-January-February (DJF). d | As in panel b, but for DJF. Stippling indicates an inter-model consensus with more than two-thirds of models showing same-signed response in the direction indicated by the colour shading. All data are the multi-model mean of CMIP6 models forced by historical forcing up to 2014, and the Shared Socioeconomic Pathway 5-8.5 (SSP5-8.5) emission scenario thereafter. ENSO-related Pacific–North American and Pacific–South American patterns are situated more to the east during eastern Pacific ENSO compared with central Pacific ENSO, and these centres tend to either strengthen or shift eastward under greenhouse warming.

Fiji, Vanuatu, Marshall Islands and Hawaii, are likely to see a larger number of tropical cyclones during El Niño events and reduced occurrences during La Niña events in the future¹²⁹.

Mechanisms influencing ENSO projection

The increase in ENSO SST variability is underpinned by a stronger air-sea coupling arising from an intensification of the equatorial Pacific upper-ocean stratification³⁶. The enhanced stratification is caused by surface-intensified warming related to increasing greenhouse-gas-induced radiative forcing and freshening owing to increased precipitation, enhancing the response of the surface mixed layer to a given wind forcing^{36,58-61}. Thus, the projected increase in ENSO SST variability is independent of faster warming in the eastern equatorial Pacific than the west, a trend that underpins the projected increase in ENSO rainfall variability²⁷. Although models with stronger warming in the eastern equatorial Pacific do tend to generate a greater increase in ENSO SST variability, and vice versa^{100,102,130}, the greater warming can result from rectification of the increased ENSO SST variability onto the mean state 101,102. Nevertheless, many factors affect the projection, such as interannual inter-basin interactions. internal variability and a too-cold equatorial Pacific cold tongue.

Inter-basin interactions

On interannual timescales, a strong appreciation has formed that Atlantic Niña (with an anomalous cooling in the equatorial east Atlantic) is conducive to a Pacific El Niño^{131,132} and an anomalous warming over the tropical North Atlantic conducive to a Pacific La Niña¹³³. Indian Ocean basin-wide warming can further contribute to a transition from El Niño to La Niña¹³⁴. The majority of models underestimate these remote impacts^{135–139}, with implications for ENSO projections^{41,140}.

For example, the projected slower warming of the Atlantic Ocean compared with the Pacific — linked to a weakened oceanic heat transport from the South Atlantic induced by a weakened Atlantic meridional overturning circulation 141 — can reduce the ability for Atlantic variability to influence ENSO events. In this situation, convection is skewed towards the Pacific sector, as atmosphere convection tends to occur over the relatively warm water¹³⁷. In addition, tropical North Atlantic SST anomalies decay faster, owing to stronger thermal damping in a warmer climate¹³⁸, and tropospheric stability increases as the lower atmosphere warms less than the upper troposphere, making anomalies induced by Atlantic convection difficult to transmit across to the Pacific¹³⁹. Both factors act to decrease the forcing of Atlantic variability on ENSO. This scenario contrasts to what has occurred in the post-1980 period, in which the Atlantic has exhibited rapid warming 90,142 with more biennial ENSO variability¹⁴³.

Although there is no inter-model consensus on how interactions between ENSO and Indian Ocean variability will change under greenhouse warming¹⁴⁴, the inter-basin warming contrasts might vary with time, inducing non-unidirectional projected changes in ENSO, as previously demonstrated in the case of a

projected relative warming between the Pacific Ocean and the Indian Ocean⁶³. However, the impact of the Atlantic Ocean and Indian Ocean future warming on future ENSO is likely to be underestimated in climate models, because the simulated present-day inter-basin interactions are underestimated^{37,41,90,94}.

Internal variability

ENSO projections are also influenced by internal variability (FIG. 1), with ENSO variability differing markedly across ensemble members of a single model, despite the same emission scenario 42-45. The inter-member spread of future ENSO variability is not completely random but dependent on past ENSO behaviour: greater initial variability over a multidecadal period is associated with smaller future variability⁴². Given that El Niño amplitude is greater than that of La Niña, ocean-to-atmosphere net heat loss during El Niño events is greater than heat gain during La Niña events145,146. The asymmetric heat flux results in a cumulative heat loss that is greater in experiments with initially stronger ENSO variability, causing the thermocline to shoal in the upper western Pacific and deepen in the EP initially. Over time, the cumulative heat loss leads to a cooling in the upper central and eastern equatorial Pacific. This cooling partly offsets the greenhouse-forced upper-ocean stratification, such that initially strong ENSO variability tends to be associated with future weak ENSO variability42.

Such relationships are also seen in models with higher ENSO nonlinearity, which tend to project weaker Niño3.4 variability and a reduced eastern equatorial Pacific warming⁵⁴. As greenhouse gas concentrations increase further, the impact of internal variability relative to the effect from greenhouse-induced change is expected to decrease, and uncertainty in the projections is expected to be dominated by inter-model differences from the 2040s onward¹⁴⁷.

Impact from the cold tongue bias

The common equatorial Pacific too-cold cold tongue and too-west extension (FIG. 3d) is further suggested to impact ENSO simulation and projected ENSO changes¹⁴⁸. For instance, the too-cold equatorial EP cold tongue can lead to a spuriously weak Bjerknes feedback that, despite being typically offset by a too-weak thermal damping^{149–151}, can hamper simulation of realistic ENSO asymmetry¹⁰², as warm anomalies are harder to grow to establish atmospheric deep convection¹⁵¹. While model selection based on realistic ENSO asymmetry is used for ENSO projections, the asymmetry in selected models is still low compared with that observed^{42,102}.

Although uncertainties remain, a scenario of increased ENSO SST variability with more frequent ENSO SST extremes continues to emerge, with intensified and shifted ENSO teleconnections. Thus, there are multiple lines of evidence that ENSO can be sensitive to anthropogenic warming.

Palaeoclimatic context of ENSO changes

Tropical Pacific interannual variability has been a feature of the Earth's climate system for millions of years¹⁵². As such, assessments of forced changes in ENSO properties

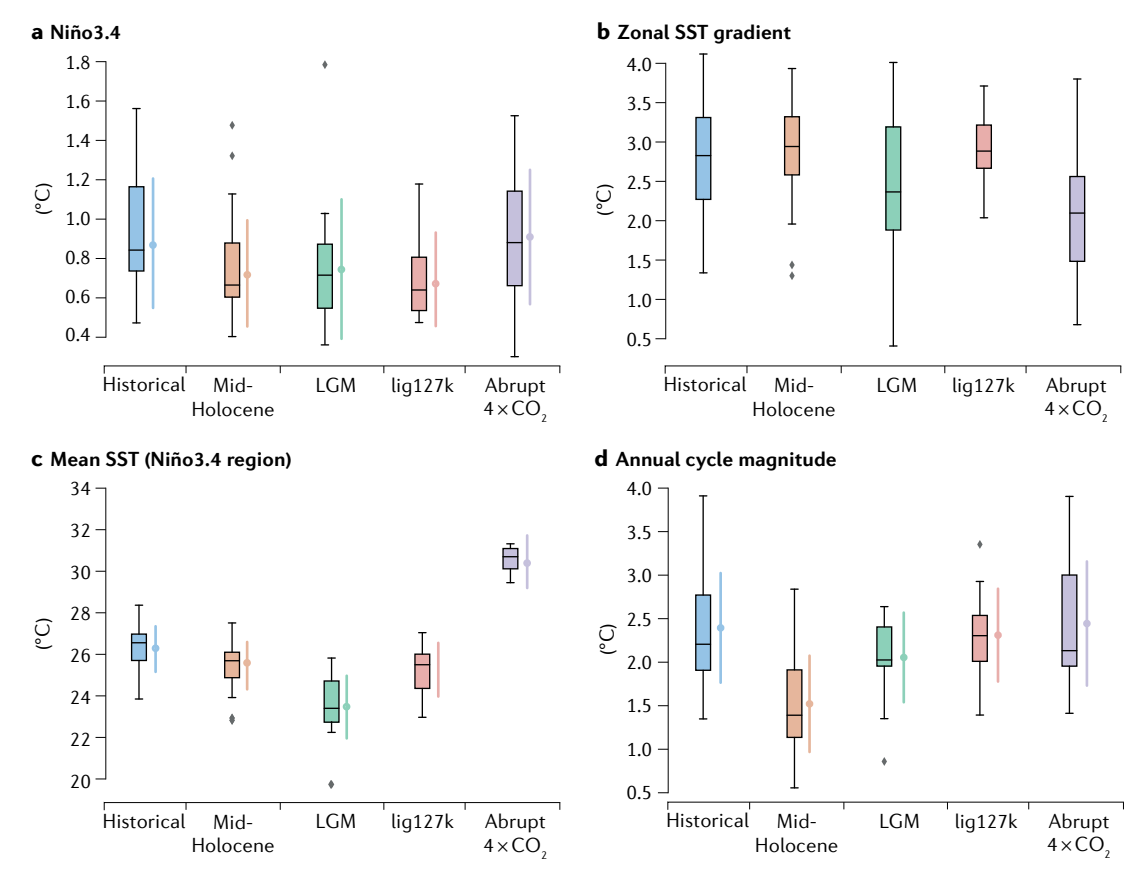


Fig. 6 | Tropical Pacific mean state and El Niño-Southern Oscillation variability in past climates. a | Niño 3.4 variability from historical (blue), mid-Holocene (orange), Last Glacial Maximum (LGM; green), last interglacial (lig127k; red) and abrupt $4 \times CO_2$ (purple) simulations as part of PMIP3/CMIP5 and PMIP4/CMIP6 (REF. 171). Box plots indicate inter-model spread and lighter point plots to the right indicate the spread when including internal variability, as estimated using 100 random 50-year samples from each model simulation (error bars draw the standard deviation of samples). b | As in panel a, but for zonal sea surface temperature (SST) gradient, estimated as the west (5°S–5°N, 100°E–180°E) minus east Pacific (5°S–5°N, 160°W–80°W) annual-mean SST difference. c | As in panel a, but for mean SST. d | As in panel a, but for annual cycle magnitude, defined as the range of monthly climatological SST in the Niño3 region (5°S–5°N, 150°W–90°W). All the palaeoclimate simulation outputs have been calendar-adjusted using the PaleoCalAdjust tool²¹⁰. While models agree that El Niño–Southern Oscillation variance was lower in past climates compared with the present-day climate, its relationship with the annual cycle, zonal SST gradient and mean SST in the central and eastern Pacific shows vast diversity in the strength and direction.

have been carried out in the context of changes in Earth's orbit, volcanic eruptions and greenhouse gas forcing, as captured in palaeoclimate datasets, observational data and climate models. Understanding past changes provides historical context for understanding contemporary and projected ENSO changes, and their relationship with mean state.

Temperature gradients and ENSO

External palaeoclimate forcings alter mean surface temperature, its zonal gradients and the depth of the thermocline, potentially affecting ENSO. However, there is no consistent relationship across different climates between ENSO and climatological SST gradients. On the one hand, foraminifera from the eastern equatorial Pacific reveal that weaker ENSO was associated with weaker zonal SST gradients in the Pliocene¹⁵³, consistent with findings from climate models^{154–156} and the Last Glacial Maximum¹⁵⁷. On the other hand, these associations oppose interpretations from other proxy data^{158–161}.

This opposite interpretation is supported by models that best simulate modern tropical Pacific climate, which frequently simulate stronger ENSO SST variance when the west-minus-east mean SST contrast is weaker, and vice versa^{162–164}.

Across different climates, no clear relationship between ENSO variance and zonal SST gradient (FIG. 6a,b) or mean SST (FIG. 6c) is exhibited in Paleoclimate Model Intercomparison Project phases 3 and 4 (PMIP3 and PMIP4) model experiments¹⁶⁵. Instead, reconstructed temperature variability in the equatorial Pacific during the Last Glacial Maximum and Pliocene suggests that ENSO strength is tied to the mean thermocline depth of the eastern equatorial Pacific and the strength of the thermocline feedback^{153,157,166}. Across multiple orbital cycles, ENSO strength correlates strongly with vertical temperature gradient¹⁶⁶. Changes in ENSO variance during the mid and early Holocene and Pliocene can thus be attributed to the vertical ocean structure in the central and eastern equatorial Pacific^{156,167–170}.

Orbital forcing and ENSO

Changes in Earth's orbital characteristics not only alter the mean climate but also modulate the seasonal amplitude of solar radiation, inducing seasonal shifts in circulation of the tropical Pacific, potentially influencing ENSO properties. However, substantial model-proxy and inter-proxy discrepancies exist.

General circulation models forced with different orbital conditions simulate, on average, a 30–40% suppression of the seasonal cycle amplitude of eastern tropical Pacific SST variability during the mid-Holocene (6,000 years ago) and a 10–20% suppression of ENSO variability^{171,172} (FIG. 6a,d). In the last interglacial, when orbital forcing was similar to that in the mid-Holocene but stronger, models show a correspondingly larger decrease in ENSO variance (FIG. 6a), but without a correspondingly larger reduction in magnitude of seasonal cycle (FIG. 6d). These suggest an orbital sensitivity of ENSO that could occur with or without a consistent change in magnitude of seasonal cycle.

Palaeoclimate proxies themselves, however, present conflicting lines of evidence of orbital sensitivity of ENSO. Records from coral¹⁷³, foraminifera¹⁶⁹, lakes and speleothems^{174–178} illustrate substantial changes in ENSO variance under orbital forcing. In contrast, other constructions reveal intervals of reduced ENSO variance that are out of phase with orbital changes in equatorial insolation¹⁷⁹. Spanning the last 7,000 years, coral-based ENSO reconstructions show no clear orbitally forced trend in ENSO variability since the mid-Holocene; instead, there appears to be a pronounced reduction in ENSO variability and the magnitude of the seasonal cycle between 3,000 and 5,000 years ago^{70,180}, a period that does not coincide with any known external forcings.

Some of these model-proxy and inter-proxy discrepancies can be due to changes in ENSO flavours and their different teleconnection patterns¹⁶⁵ that are not resolved by individual proxies. For example, the mid-Holocene ENSO reduction was most pronounced in the eastern equatorial Pacific, whereas CP ENSO events remained relatively unaffected or even slightly increased¹⁶⁸. Given these discrepancies, it appears that ENSO's sensitivity to orbital forcing remains highly uncertain⁷¹.

Volcanic forcing and ENSO

Improved understanding of volcanic forcing on ENSO variability also offers opportunities to better assess the role of natural and anthropogenic aerosols in ENSO variability in present and future climates¹⁸¹. However, there is currently much uncertainty surrounding the impact of volcanic forcing on ENSO. For instance, in some cases, the probability of El Niño events increases in the year following an eruption^{34,182-186}, whereas in others, a weak La Niña response^{187,188} or no clear signals^{189–191} emerge. The cause of these differences can be related, in part, to the multiple factors involved, including the Pacific-wide initial conditions, the location and season of the eruption, and the spatial structure of the volcanic aerosols^{192–196}. For example, Northern Hemisphere tropical eruptions typically generate an El Niño-like response, while Southern Hemisphere tropical eruptions induce a La Niña-like response¹⁹⁵. A uniform negative radiative

forcing over the tropics further induces a La Nina-like response, contrary to the expectation from the ocean dynamical thermostat mechanism⁸⁵. Thus, reducing proxy dating uncertainties and accounting for the latitude and timing of eruptions is important for assessing ENSO's sensitivity to aerosol forcing.

Uncertainty in palaeoclimate records

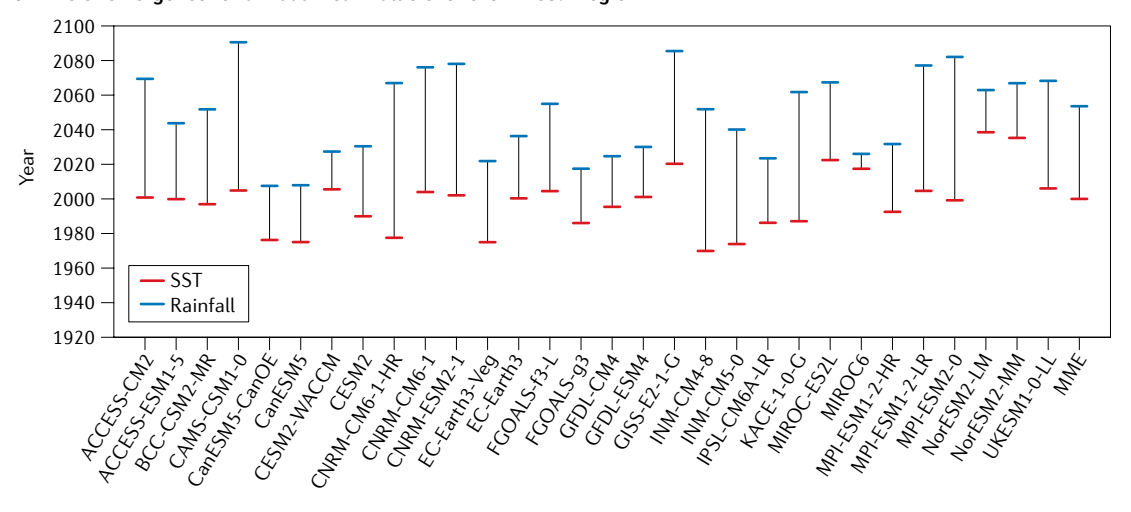
Limitations of palaeoclimate reconstruction exist⁷¹, hindering interpretation of the relationship of ENSO with mean circulation and with orbital forcing. These include nonlinearities and non-stationarity in teleconnected proxy records197, aliasing of natural ENSO variability and difficulty in separating the impacts of ENSO, its diversity and seasonal cycle changes in both direct and teleconnected or indirect ENSO proxies. Further, most of these proxy records reflect ENSO-related temperature, rainfall and salinity, which can lead to nonlinearities and non-stationarity in the recorded signal¹⁹⁷. In addition, regional topography and mesoscale circulation processes can lead to departure of regional signals from the expected large-scale signature of ENSO events¹⁹⁸. Thus, the observed interannual variance in land-based hydroclimate or coral-based records likely reflect a change in ENSO-related temperature and hydrological variability combined, ENSO diversity and the regional or large-scale teleconnections^{168,199}.

Despite the limitations, palaeoclimate reconstructions, when carefully combined with dynamical understanding, offer the ability to ground-truth model simulations and to inform targeted experiments for distinguishing underlying mechanisms. However, it is challenging to use past climates as exact analogues or reverse analogues for centennial-scale anthropogenic climate change due to issues such as coupling of the zonal and vertical gradients, the lack of a clear consistent relationship between mean circulation and ENSO variability in palaeoclimate records and model experiments, and incomparability between available climate proxies that resolve equilibrium conditions and the transient response to greenhouse warming that we are interested in. Nevertheless, the link between enhanced vertical temperature gradients with increased ENSO variability appears to operate in many past climates and in the projected twenty-first century climate.

Summary and future perspectives

There is an emerging inter-model consensus among models that capture the distinction between EP and CP ENSO events, that ENSO SST variability is likely to increase, in turn, increasing the frequency of extreme El Niño and La Niña events in terms of SST anomaly magnitude; this consensus is stronger in CMIP6 compared with CMIP5. Associated with this change is an intensification and eastward shift of equatorial Pacific rainfall responses and extratropical teleconnections. These projected changes are consistent with lines of palaeoclimatic evidence that suggest that ENSO variability has increased since the 1950s compared with past centuries, and that, on long timescales, ENSO variability strength increases with the equatorial Pacific vertical temperature gradient. In addition, future changes in ENSO SST

a Time of emergence for annual-mean value over the Niño3.4 region



b Time of emergence for interannual variability over the Niño3.4 region

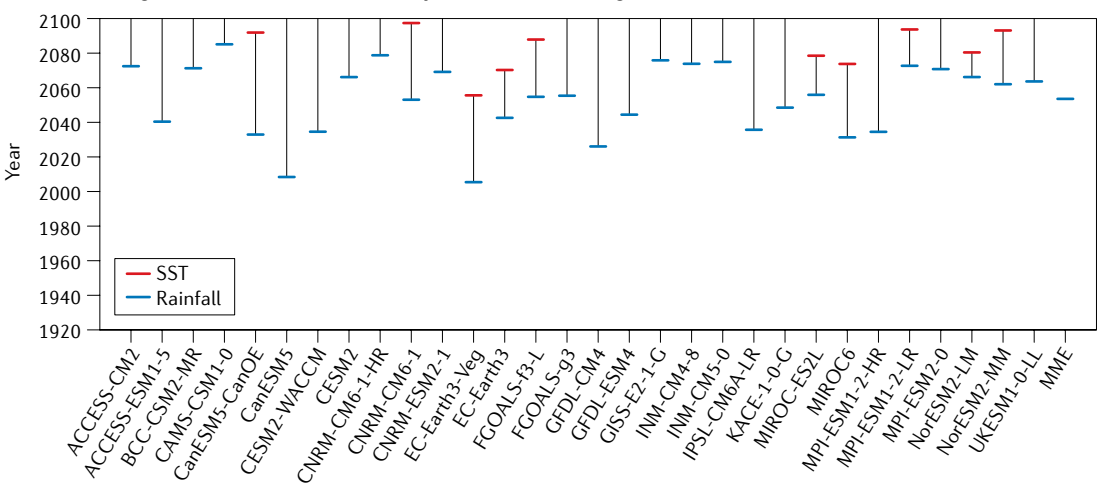


Fig. 7 | Time of emergence of climate change signals. a | The time of emergence (ToE; the year when anthropogenic signals emerge from noise) of annual-mean sea surface temperature (SST; red) and rainfall (blue) over the Niño3.4 region for each CMIP6 model and the multi-model ensemble (MME) mean. Signals are obtained by regressing time series of 150 annual-mean values in each grid point onto a smoothed version of the tropical mean (30°S–30°N) by fitting a fourth-order polynomial²⁰⁷. The ToE is defined as the year when the signal-to-noise ratio exceeds 1. b | The ToE for interannual variability in SST (red) and precipitation (blue). Signals are obtained by regressing time series of 30-year running standard deviation of anomalies quadratically detrended for each 30-year period onto time series of 30-year running climatology of the tropical mean similarly smoothed by fitting a fourth-order polynomial. For illustration, the ToE for interannual variability is defined as when the signal-to-noise ratio exceeds 1.5. In both cases, 'signals' are derived from CMIP6 models under historical forcing and the Shared Socioeconomic Pathway 5-8.5 (SSP5-8.5) emission scenario over the 1850 to 2099 period (150 years) and 'noise' from a 500-year pre-industrial experiment of the respective model as the standard deviation of annual-mean values. The ToE for interannual rainfall variability is sooner than that for interannual SST variability, whereas the ToE for the annual-mean rainfall is later than the annual-mean SST.

are not simply a function of emission scenarios but are influenced by the past history of ENSO variability.

However, uncertainties remain. On multidecadal timescales, confidence is reduced by the disparity between the projected west-minus-east zonal SST gradient weakening and the observed strengthening over the past several decades^{38,40,86}, model cold tongue biases and inter-basin interactions that are too weak^{37,41,94,95}. On interannual timescales, simulated inter-basin teleconnections are also too weak, influencing ENSO impacts on the Atlantic and/or Indian oceans, as well as the impacts of the Atlantic and/or Indian oceans on ENSO^{41,136,138,139}.

It is not clear how these two-way interactions will change and how the changes will affect ENSO.

Further, ENSO is coupled with and influenced by other variability at higher latitudes of the Pacific. For example, El Niño events are preceded by and coupled with warm anomalies of the North Pacific meridional mode^{200–202}, and forced by southerly jets from the south-western Pacific²⁰³. There is incomplete knowledge of how these tropical–extratropical connections are simulated in climate models and how they will respond to greenhouse warming.

In terms of ENSO properties, little is known about how other essential characteristics of ENSO could change, such as the termination and onset of ENSO events, coupling between stochastic noise and ENSO, and interactions between ENSO and the annual cycle^{17,71}. In regards to ENSO physics, the role of eddy-induced oceanic heat transport and oceanic turbulent mixing is not well understood or parameterized²⁰⁴, nor are sub-grid atmosphere process such as atmospheric convection, cloud formation and their coupling to other ENSO processes²⁰⁵.

Nevertheless, coordinated community efforts like CMIP and advances in computational power will continue to facilitate progress. Large-ensemble simulations²⁰⁶, long control climate simulations and high-resolution climate modelling (0.1° in horizontal resolution for the ocean model component) show great promise in addressing key questions about ENSO in a warmer world.

When the 'signal' of increased ENSO SST variability or the changing mean state might clearly emerge from the background noise of internal variability, or whether such a signal will ever be detectable in a single realization of the real world, is key open question. Long, multi-century control simulations of the climate system provide a wide range of realizations for this assessment. The concept of the 'time of emergence' for SST and precipitation signals in the equatorial Pacific, referenced to pre-industrial conditions, indicate when it should be possible to detect these signals against the background noise of natural internal variability²⁰⁷. For changes in mean SST in the Niño3.4 region under the most aggressive greenhouse gas emission scenario, the time of emergence should have been around the turn of the twenty-first century (FIG. 7a). However, the discrepancy between models and observations and the inter-model spread prevent a clear greenhouse gas forced mean state temperature change from being observed. For changes in mean precipitation in the Niño3.4 region, the signal might not emerge until mid-twenty-first century. Conversely, the situation for SST and precipitation variability is reversed; rainfall variability emerges sooner than SST variability (FIG. 7b). The earlier emergence of rainfall variability confirms the robust signal of more extreme El Niño events in the future when measured by a rainfall threshold²⁷. These findings suggest that ENSO changes should be detectable within the twenty-first century; however, the time of emergence for teleconnections impacting ENSO-affected regions awaits investigation.

Large-ensemble experiments within a single model have led to the realization that internal variability $^{42-45}$ and

the butterfly effect⁴² influence projected ENSO change. Available simulations suggest that, while responding to greenhouse warming, ENSO constantly self-regulates in accordance with its own past behaviour42. That is, high past variability takes heat out of the upper equatorial Pacific Ocean, offsetting greenhouse-warming-induced upper-ocean stratification and weakening ENSO's response, which, in turn, sets up for a strong subsequent response by reducing oceanic heat loss. The self-regulation raises an issue of whether there is a deterministic equilibrium ENSO response to greenhouse warming in a single realization. In other words, is ENSO change quantifiable in a given window of time in the future? Large-ensemble experiments with multiple models offer an opportunity to test the robustness of this self-regulating behaviour and to inspire theoretical models of the associated process.

Furthermore, high-resolution climate models not only better resolve ENSO teleconnection patterns, intensity and associated climate extremes at regional scales, subgrid ocean and atmosphere processes but also allow explicit definition of previously unresolved physical processes. One example is heat transport induced by equatorial Pacific oceanic eddies (such as tropical instability waves) on the mean state heat balance of the equatorial Pacific. For the equatorial Pacific mean state, eddy-induced heat transport represents a substantial heat source comparable with heat uptake from the atmosphere²⁰⁸. The eddy-induced heat source is reduced during El Niño but increases during La Niña, constraining ENSO amplitude²⁰⁹ while substantially contributing to ENSO irregularity and predictability²⁰⁴. Given that such eddy effects are not resolved by low-resolution climate models, it is likely that the simulated cold tongue bias and other ENSO property biases¹⁴⁹ in CMIP models could be due, in part, to the absence of the eddy process. Thus, high-resolution ENSO modelling offers a path forward for substantial improvement in ENSO simulations and projections.

Thus, despite rapid progress, fully understanding ENSO responses to greenhouse warming is far from resolved. The coming decade offers opportunities for substantial advances as community efforts strengthen, cutting-edge ideas emerge and realistic models become available. The robust scientific process, whereby debates inspire research and progress identifies new issues, will propel the field forward.

Published online: 17 August 2021

- Philander et al. Unstable air-sea interactions in the tropics. J. Atmos. 41, 604–613 (1984).
- Ropelewski, C. F. & Halpert, M. S. Global and regional scale precipitation patterns associated with the El Niño/Southern Oscillation. Mon. Weather Rev. 115, 1606–1626 (1987).
- McPhaden et al. ENSO as an integrating concept in earth science. Science 314, 1740–1745 (2006).
- L'Heureux, M. L. et al. Observing and predicting the 2015/16 El Niño. Bull. Am. Meteorol. Soc. 98, 1363–1382 (2017).
- Santoso, A., McPhaden, M. J. & Cai, W. The defining characteristics of ENSO extremes and the strong 2015/16 El Niño. Rev. Geophys. 55, 1079–1129 (2017).
- Bjerknes, J. Atmospheric teleconnections from the equatorial Pacific. *Mon. Weather. Rev.* 97, 163–172 (1969).

- Cai, W. et al. Climate impacts of the El Nino–Southern Oscillation on South America. Nat. Rev. Earth Environ. 1, 215–231 (2020).
- Ashok, K., Behera, S. K., Rao, S. A., Weng, H. Y. & Yamagata, T. El Niño Modoki and its possible teleconnection. *J. Geophys. Res.* 112, C11007 (2007).
 Defines a type of El Niño with maximum SST anomaly in the equatorial CP atmospheric teleconnection different from El Niño with anomaly centre in the equatorial EP.
- Valle, C. A. et al. The impact of the 1982–1983 El Niño-Southern Oscillation on seabirds in the Galapagos Islands, Ecuador. J. Geophys. Res. Oceans 92, 14,437–14,444 (1987).
- Holbrook, N. J. et al. Keeping pace with marine heatwaves. *Nat. Rev. Earth Environ.* 1, 482–493 (2020).

- Glynn, P. W. & de Weerdt, W. H. Elimination of two reef-building hydrocorals following the 1982–83 El Niño. Science 253, 69–71 (1991).
- Jonkman, S. N. Global perspectives on loss of human life caused by floods. *Nat. Hazards* 34, 151–175 (2005).
- Kunii, O., Nakamura, S., Abdur, R. & Wakai, S. The impact on health and risk factors of the diarrhoea epidemics in the 1998 Bangladesh floods. *Public Health* 116, 68–74 (2002).
- del Ninno, C. & Dorosh, P. A. Averting a food crisis: private imports and public targeted distribution in Bangladesh after the 1998 flood. *Agric. Econ.* 25, 337–346 (2001).
- McPhaden, M. J., Santoso, A., & Cai, W. (eds) El Niño Southern Oscillation in a Changing Climate Vol. 253 (Wiley, 2020).

- Collins, M. et al. The impact of global warming on the tropical Pacific Ocean and El Niño. *Nat. Geosci.* 3, 391–397 (2010).
- 17. Cai, W. et al. ENSO and greenhouse warming. *Nat. Clim. Change* **5**, 849–859 (2015).
- Jin, F.-F. & Neelin, J. D. Modes of interannual tropical ocean-atmosphere interaction — A unified view. Part I: Numerical results. J. Atmos. 50, 3477–3503 (1993).
- An, S.-I. & Jin, F.-F. An eigen analysis of the interdecadal changes in the structure and frequency of ENSO mode. *Geophys. Res. Lett.* 27, 1573–1576 (2000).
- Fedorov, A. V. & Philander, S. G. A stability analysis of tropical ocean-atmosphere interactions: Bridging measurements and theory for El Niño. *J. Clim.* 14, 3086–3101 (2001).
- IPCC. Climate Change 2013: The Physical Science Basis. Contribution of Working Group I to the Fifth Assessment Report of the Intergovernmental Panel on Climate Change (eds Stocker, T. F. et al) 1535 pp (Cambridge Univ. Press, 2013).
- 22. IPCC. Global Warming of 1.5 °C. An IPCC Special Report on the impacts of global warming of 1.5 °C above pre-industrial levels and related global greenhouse gas emission pathways, in the context of strengthening the global response to the threat of climate change, sustainable development, and efforts to eradicate poverty (eds Masson-Delmotte, V. et al) https://www.ipcc.ch/sr15/(2018).
- Meehl, G. A., Brantstator, G. W. & Washington, W. M. Tropical Pacific interannual variability and CO₂ climate change. *J. Clim.* 6, 42–63 (1993).
- Tett, S. Simulation of El Niño-Southern Oscillation-like variability in a global AOGCM and its response to CO₂ increase. *J. Clim.* 8, 1473–1502 (1995).
- Power, S. B., Delage, F., Chung, C., Kociuba, G. & Keay, K. Robust twenty-first century projections of El Niño and related precipitation variability. *Nature* 502, 541–545 (2013).
- Yun, K. S. et al. Increasing ENSO-rainfall variability due to changes in future tropical temperature-rainfall relationship. *Commun. Earth Environ.* 2, 43 (2021).
- Cai, W. et al. Increasing frequency of extreme El Niño events due to greenhouse warming. *Nat. Clim. Change* 4, 111–116 (2014).
- 28. Wang, G. et al. Continued increase of extreme El Niño frequency long after 1.5 C warming stabilization. Nat. Clim. Change 7, 568–572 (2017). Finds that extreme El Niño frequency continues to increase for up to a century after global warming is halted at 1.5 °C above pre-industrial level.
- Cai, W. et al. More extreme swings of the South Pacific convergence zone due to greenhouse warming. *Nature* 488, 365–369 (2012).
- Brown, J. R. et al. South Pacific Convergence Zone dynamics, variability and impacts in a changing climate. Nat. Rev. Earth Environ. 1, 530–543 (2020).
- Santoso, A. et al. Late-twentieth-century emergence of the El Niño propagation asymmetry and future projections. *Nature* 504, 126–130 (2013).
- Cai, W. et al. Increased frequency of extreme La Niña events under greenhouse warming. *Nat. Clim. Change* 5, 132–137 (2015).
- 33. Grothe, P. R. et al. Enhanced El Niño—Southern oscillation variability in recent decades. Geophys. Res. Lett. 47, e2019GL083906 (2020). Shows decreased ENSO variance 3,000–5,000 years ago and ENSO strengthening in the last five decades, using a new ensemble of fossil coral oxygen isotope records from the central equatorial Pacific.
- McGregor, S., Timmermann, A. & Timm, O. A unified proxy for ENSO and PDO variability since 1650. Clim. Past. 6, 1–17 (2010).
- McGregor, H. et al. A weak El Niño/Southern
 Oscillation with delayed seasonal growth around
 4,300 years ago. Nat. Geosci. 6, 949–953 (2013).
- Cai, W. et al. Increased variability of eastern Pacific El Niño under greenhouse warming. Nature 564, 201–206 (2018).
- Luo, J.-J., Wang, G. & Dommenget, D. May common model biases reduce CMIPS's ability to simulate the recent Pacific La Niña-like cooling? Clim. Dyn. 50, 1335–1351 (2018).
- Coats, S. & Karnauskas, K. B. A role for the equatorial undercurrent in the ocean dynamical thermostat. *J. Clim.* 31, 6245–6261 (2018).
- Seager, R. et al. Strengthening tropical Pacific zonal sea surface temperature gradient consistent with rising greenhouse gases. *Nat. Clim. Change* 9, 517–522 (2019).

- 40. Chung, E. S. et al. Reconciling opposing Walker circulation trends in observations and model projections. Nat. Clim. Change 9, 405–412 (2019). Shows a reduced strengthening of the Pacific Walker circulation during recent decades in satellite observations compared with reanalysis products and a dominant role of internal variability in the strengthening.
- 41. Cai, W. et al. Pantropical climate interactions. *Science* **363**, eaav4236 (2019).
- Cai, W. et al. Butterfly effect and a self-modulating El Niño response to global warming. *Nature* 585, 68–73 (2020).
 - Demonstrates that ENSO exhibits a self-regulating behaviour such that future variability is shaped by its past, thus, modulating the effect of greenhouse forcing.

 Maher, N., Matei, D., Milinski, S. & Marotzke, J.
- Maher, N., Matei, D., Milinski, S. & Marotzke, J. ENSO change in climate projections: Forced response or internal variability? *Geophys. Res. Lett.* 45, 11,390–11,398 (2018).
- Zheng, X.-T., Hui, C. & Yeh, S. W. Response of ENSO amplitude to global warming in CESM large ensemble: uncertainty due to internal variability. *Clim. Dyn.* 50, 4019–4035 (2018).
- Ng, B., Cai, W., Cowan, T. & Bi, D. Impacts of low-frequency internal climate variability and greenhouse warming on El Niño–Southern Oscillation. J. Clim. 34, 2205–2218 (2021).
- Fu, C. & Fletcher, J. O. Two patterns of equatorial warming associated with El Niño. *Chin. Sci. Bull.* 30, 1360–1364 (1985).

Shows that there are two types of equatorial warming associated with El Niño.

- Fu, C., Diaz, H. F. & Fletcher, J. O. Characteristics of the response of sea surface temperature in the central Pacific associated with warm episodes of the Southern Oscillation. Mon. Weather Rev. 114, 1716–1738 (1986).
- Capotondi, A. et al. Understanding ENSO diversity. Bull. Am. Meteorol. Soc. 96, 921–938 (2015).
- Capotondi, A., Wittenberg, A. T., Kug, J.-S., Takahashi, K. & McPhaden, M. J. ENSO Diversity, in El Niño Southern Oscillation in a Changing Climate (eds McPhaden, M. J., Santoso, A. & Cai, W.) (AGU, 2020).
- Takahashi, K. & Dewitte, B. Strong and moderate nonlinear El Niño regimes. Clim. Dyn. 46, 1627–1645 (2016).
- 51. Timmermann, A. et al. El Niño—southern oscillation complexity. *Nature* **559**, 535–545 (2018).
- Dommenget, D., Bayr, T. & Frauen, C. Analysis of the non-linearity in the pattern and time evolution of El Niño Southern Oscillation. *Clim. Dyn.* 40, 2825–2847 (2013).
- Takahashi, K., Montecinos, A., Goubanova, K. & Dewitte, B. ENSO regimes: Reinterpreting the canonical and Modoki El Niño. *Geophys. Res. Lett.* 38, L10704 (2011).
- Karamperidou, C., Jin, F.-F. & Conroy, J. L. The importance of ENSO nonlinearities in tropical Pacific response to external forcing. *Clim. Dyn.* 49, 2695–2704 (2017).
- Philip, S. Y. & van Oldenborgh, G. J. Shifts in ENSO coupling processes under global warming. *Geophys. Res. Lett.* 33, L11704 (2006).
- Jin, F.-F., Kim, S. T. & Bejarano, L. A coupled-stability index for ENSO. *Geophys. Res. Lett.* 33, L23708 (2006).
- Kim, S. T. & Jin, F.-F. An ENSO stability analysis. Part II: results from the twentieth and twenty-first century simulations of the CMIP3 models. *Clim. Dyn.* 36, 1609–1627 (2011).
- Carréric, A. et al. Change in strong Eastern Pacific El Niño events dynamics in the warming climate. Clim. Dyn. 54, 901–918 (2020).
- Dewitte, B., Yeh, S.-W., Moon, B.-K., Cibot, C. & Terray, L. Rectification of the ENSO variability by interdecadal changes in the equatorial background mean state in a CGCM simulation. *J. Clim.* 20, 2002–2021 (2007).
- Timmermann, A. et al. Increased El Niño frequency in a climate model forced by future greenhouse warming *Nature* 398, 694–697 (1999).
 Thual, S., Dewitte, B., An, S.-I. & Ayoub, N. Sensitivity
- 61. Thual, S., Dewitte, B., An, S. I. & Ayoub, N. Sensitivit of ENSO to stratification in a recharge—discharge conceptual model. J. Clim. 4, 4331–4348 (2011). Refines the theoretical framework showing intensified ocean—atmosphere coupling as the mean upper-ocean stratification increases.
- Zhang, Q., Guan, Y. & Yang, H. ENSO amplitude change in observation and coupled models. *Adv. Atmos. Sci.* 25, 361–366 (2008).

- Kim, S. T. et al. Response of El Niño sea surface temperature variability to greenhouse warming. *Nat. Clim. Change* 4, 786–790 (2014).
- Geng, T., Cai, W. & Wu, L. Two types of ENSO varying in tandem facilitated by nonlinear atmospheric convection. *Geophys. Res. Lett.* 47, e2020GL088784 (2020)
- Capotondi, A. & Sardeshmukh, P. D. Is El Niño really changing? Geophys. Res. Lett. 44, 8548–8556 (2017)
- Wang, B. et al. Historical change of El Niño properties sheds light on future changes of extreme El Niño. Proc. Natl Acad. Sci. USA 116, 22512–22517 (2019).
- Kennedy, J. J. A review of uncertainty in in situ measurements and data sets of sea surface temperature. Rev. Geophys. 52, 1–32 (2014).
- 68. Li, J. et al. El Niño modulations over the past seven centuries. *Nat. Clim. Change* **3**, 822–826 (2013).
- Liu, Y. et al. Recent enhancement of central Pacific El Niño variability relative to last eight centuries. Nat. Commun. 8, 15386 (2017).
- Cobb, K. M. et al. Highly variable El Niño-southern oscillation throughout the Holocene. *Science* 339, 67-70 (2013).
- Karamperidou, C. et al. ENSO in a Changing Climate: Challenges, Paleo-Perspectives, and Outlook, in El Niño Southern Oscillation in a Changing Climate (eds McPhaden, M. J., Santoso, A. & Cai, W.) (AGU, 2020).
- Freund, M. et al. Higher frequency of Central Pacific El Niño events in recent decades relative to past centuries. *Nat. Geosci.* 12, 450–455 (2019).
- Rayner, N. A. et al. Global analyses of sea surface temperature, sea ice, and night marine air temperature since the late nineteenth century. *J. Geophys. Res.* 108, 4407 (2003).
- Huang, B. et al. Extended reconstructed sea surface temperature, version 5 (ERSSTv5): upgrades, validations, and intercomparisons. *J. Clim.* 30, 8179
 –8205 (2017).
- Ishii, M., Shouji, A., Sugimoto, S. & Matsumoto, T. Objective analyses of sea-surface temperature and marine meteorological variables for the 20th century using ICOADS and the Kobe collection. *Int. J. Climatol.* 25, 865–879 (2005).
- Slivinski, L. C. et al. Towards a more reliable historical reanalysis: Improvements for version 3 of the Twentieth Century Reanalysis system. Q. J. R. Meteorol. Soc. 145, 2876–2908 (2019).
- Poli, P. et al. ERA-20C: An atmospheric reanalysis of the twentieth century. *J. Clim.* 29, 4083–4097 (2016).
- Kobayashi, S. et al. The JRA-55 reanalysis: General specifications and basic characteristics. *J. Meteorol* Soc. Jpn. Ser. II 93, 5–48 (2015).
- Lian, T., Chen, D., Ying, J., Huang, P. & Tang, Y. Tropical Pacific trends under global warming: El Niño-like or La Niña-like? *Natl Sci. Rev.* 5, 810–812 (2018).
- Cai, W. et al. ENSO Response to Greenhouse Forcing, in El Niño Southern Oscillation in a Changing Climate (eds McPhaden, M. J., Santoso, A. & Cai, W.) (AGU, 2020).
- Knutson, T. R. & Manabe, S. Time-mean response over the tropical Pacific to increased CO₂ in a coupled ocean-atmosphere model. *J. Clim.* 8, 2181–2199 (1995).
- Liu, Z., Vavrus, S., He, F., Wen, N. & Zhong, Y. Rethinking tropical ocean response to global warming: the enhanced equatorial warming. *J. Clim.* 18, 4684–4700 (2005).
- Xie, S. et al. Global warming pattern formation: sea surface temperature and rainfall. *J. Clim.* 23, 966–986 (2010).
- Meehl, G. & Washington, W. El Niño-like climate change in a model with increased atmospheric CO₂ concentrations. *Nature* 382, 56–60 (1996).
- 85. Clement, A. C., Seager, R., Cane, M. A. & Zebiak, S. E. An ocean dynamical thermostat. J. Clim. 9, 2190–2196 (1996).
- Watanabe, M. et al. Enhanced warming constrained by past trends in equatorial Pacific sea surface temperature gradient. *Nat. Clim. Change* 11, 33–37 (2021).
- Kociuba, G. & Power, S. B. Inability of CMIP5 models to simulate recent strengthening of the Walker circulation: Implications for projections. *J. Clim.* 28, 20–35 (2015).
- Coats, S. & Karnauskas, K. B. Are simulated and observed twentieth century tropical Pacific sea surface temperature trends significant relative to internal variability? *Geophys. Res. Lett.* 44, 9928–9937 (2017).

REVIEWS

- Zhang, L. et al. Indian Ocean warming trend reduces Pacific warming response to anthropogenic greenhouse gases: An interbasin thermostat mechanism. *Geophys. Res. Lett.* 46, 10882–10890 (2019).
- McGregor, S. et al. Recent Walker circulation strengthening and Pacific cooling amplified by Atlantic warming. Nat. Clim. Change 4, 888–892 (2014).
- Meehl, G. A. et al. Atlantic and Pacific tropics connected by mutually interactive decadal-timescale processes. *Nat. Geosci.* 14, 36–42 (2021).
 Li, X., Xie, S.-P., Gille, S. T. & Yoo, C. Atlantic-induced
- Li, X., Xie, S.-P., Gille, S. T. & Yoo, C. Atlantic-induce pan-tropical climate change over the past three decades. *Nat. Clim. Change* 6, 275–279 (2016).
- Lee, S.-K., Kim, D., Foltz, G. R. & Lopez, H. Pantropical response to global warming and the emergence of a La Niña-like mean state trend. *Geophys. Res. Lett.* 47, e2019GL086497 (2020).
- McGregor, S. et al. Model tropical Atlantic biases underpin diminished Pacific decadal variability. Nat. Clim. Change 8, 493–498 (2018).
- Kajtar, J. B., Santoso, A., McGregor, S., England, M. H. & Baillie, Z. Model under-representation of decadal Pacific trade wind trends and its link to tropical Atlantic bias. Clim. Dyn. 50, 1471–1484 (2018).
- Li, C., Dommenget, D. & McGregor, S. Trans-basin Atlantic-Pacific connections further weakened by common model Pacific mean SST biases. Nat. Commun. 11, 5677 (2020).
- 97. Stuecker, M. F. et al. Strong remote control of future equatorial warming by off-equatorial forcing. Nat. Clim. Change 10, 124–129 (2020). Demonstrates opposite-signed feedbacks in the equatorial and off-equatorial regions to greenhouse gas forcing via coupled interactions between clouds, Hadley circulation and oceanic subtropical cells.
- Heede, U. K., Fedorov, A. V. & Burls, N. J. Time scales and mechanisms for the tropical pacific response to global warming: a tug of war between the ocean thermostat and weaker Walker. *J. Clim.* 33, 6101–6118 (2020).
 Cai, W. & Whetton, P. H. Evidence for a time-varving
- Cai, W. & Whetton, P. H. Evidence for a time-varying pattern of greenhouse warming in the Pacific Ocean. Geophys. Res. Lett. 27, 2577–2580 (2000).
- 100. Zheng, X.-T., Xie, S.-P., Lv, L. H. & Zhou, Z. Q. Intermodel uncertainty in ENSO amplitude change tied to Pacific Ocean warming pattern. *J. Clim.* 29, 7265–7279 (2016).
- Kohyama, T., Hartmann, D. L. & Battisti, D. S. La Niña—like mean-state response to global warming and potential oceanic roles. J. Clim. 30, 4207–4225 (2017).
- 102. Hayashi, M., Jin, F.-F. & Stuecker, M. F. Dynamics for El Niño-La Niña asymmetry constrain equatorial-Pacific warming pattern. Nat. Commun. 11, 4230 (2020).
- 103. Ying, J., Huang, P., Lian, T. & Tan, H. Understanding the effect of an excessive cold tongue bias on projecting the tropical Pacific SST warming pattern in CMIP5 models. Clim. Dyn. 52, 1805–1818 (2018).
- 104. Taschetto, A. S. et al. Cold tongue and warm pool ENSO events in CMIPS: mean state and future projections. *J. Clim.* 27, 2861–2885 (2014).
 105. DiNezio, P. N. et al. Mean climate controls on the
- 105. DiNezio, P. N. et al. Mean climate controls on the simulated response of ENSO to increasing greenhouse gases. J. Clim. 25, 7399–7420 (2012).
- Dommenget, D. & Vijayeta, A. Simulated future changes in ENSO dynamics in the framework of the linear recharge oscillator model. *Clim. Dyn.* 53, 4233–4248 (2019).
- 107. Chen, C., Cane, M. A., Wittenberg, A. T. & Chen, D. ENSO in the CMIP5 simulations: Life cycles, diversity, and responses to climate change. *J. Clim.* 30, 775–801 (2017).
- Wang, G., Cai, W. & Santoso, A. Stronger increase in the frequency of extreme convective El Niño than extreme warm El Niño under greenhouse warming. *J. Clim.* 33, 675–690 (2020).
 Zheng, X.-T., Hui, C., Xie, S.-P., Cai, W. & Long, S.-M.
- 109. Zheng, X.-T., Hui, C., Xie, S.-P., Cai, W. & Long, S.-M. Intensification of El Niño rainfall variability over the tropical Pacific in the slow oceanic response to global warming. *Geophys. Res. Lett.* 46, 2253–2260 (2019).
- Fredriksen, H.-B., Berner, J., Subramanian, A. C. & Capotondi, A. How does El Niño–Southern Oscillation change under global warming — A first look at CMIP6. Geophys. Res. Lett. 47, e2020GL0990640 (2020).
- Planton, Y. et al. Evaluating climate models with the CLIVAR 2020 ENSO metrics package. Bull. Am. Meteorol. Soc. 102, E193–E217 (2021).
- 112. McKenna, S., Santoso, A., Sen Gupta, A., Taschetto, A. & Cai, W. Indian Ocean Dipole in CMIP5 and CMIP6:

- characteristics, biases, and links to ENSO. *Sci. Rep.* **10**. 11500 (2020).
- 10, 11500 (2020).

 113. Zhou, Z.-Q., Xie, S.-P., Zheng, X.-T., Liu, Q. & Wang, H. Global warming-induced changes in El Niño teleconnections over the North Pacific and North America. *J. Clim.* 27, 9050–9064 (2014).
- Bonfils, C. J. et al. Relative contributions of mean-state shifts and ENSO-driven variability to precipitation changes in a warming climate. *J. Clim.* 28, 9997–10013 (2015).
- 115. Huang, P. & Chen, D. Enlarged asymmetry of tropical Pacific rainfall anomalies induced by El Niño and La Niña under global warming. J. Clim. 30, 1327–1343 (2017).
- 116. Chen, Z., Gan, B., Wu, L. & Jia, F. Pacific-North American teleconnection and North Pacific Oscillation: historical simulation and future projection in CMIP5 models. Clim. Dyn. 50, 4379–4403 (2018).
- 117. Yeh, S.-W. et al. Atmospheric teleconnections and their response to greenhouse gas forcing. *Rev. Geophys.* 56, 185–206 (2018).
- Michel, C. et al. The change in the ENSO teleconnection under a low global warming scenario and the uncertainty due to internal variability. *J. Clim.* 33, 4871–4889 (2020).
- 119. Sohn, B.-J., Yeh, S.-W., Lee, A. & Lau, W. K. M. Regulation of atmospheric circulation controlling the tropical Pacific precipitation change in response to CO₂ increases. *Nat. Commun.* 10, 1108 (2019).
- 120. Yan, Z. et al. Eastward shift and extension of ENSO-induced tropical precipitation anomalies under global warming. *Sci. Adv.* 6, eaax4177 (2020).
 121. Beverley, J. D., Collins, M., Lambert, F. H. &
- Beverley, J. D., Collins, M., Lambert, F. H. & Chadwick, R. Future changes to El Niño teleconnections over the North Pacific and North America. *J. Clim.* https://doi.org/10.1175/JCLI-D-20-0877.1 (2021).
 Stevenson, S. L. Significant changes to ENSO
- 122. Stevenson, S. L. Significant changes to ENSO strength and impacts in the twenty-first century: results from CMIP5. *Geophy. Res. Lett.* 39, L17703 (2012)
- Tedeschi, R. G. & Collins, M. The influence of ENSO on South American precipitation: simulation and projection in CMIP5 models. *Int. J. Climatol.* 37, 3319–3339 (2017).
- 124. Power, S. B. & Delage, F. P. D. El Niño—Southern Oscillation and associated climatic conditions around the world during the latter half of the twenty-first century. J. Clim. 31, 6189–6207 (2018).
- 125. Perry, S. J., McGregor, S., Sen Gupta, A. & England, M. H. Future changes to El Niño—Southern Oscillation temperature and precipitation teleconnections. *Geophys. Res. Lett.* 44, 10608–10616 (2017).
- 126. Lyon, B. The strength of El Niño and the spatial extent of tropical drought. *Geophys. Res. Lett.* 3, L21204 (2004).
- Delagé, F. P. D. & Power, S. B. The impact of global warming and the El Niño-Southern Oscillation on seasonal precipitation extremes in Australia. Clim. Dyn. 54, 4367–4377 (2020).
- 128. Lin, I.-I. et al. ENSO and Tropical Cyclones, in El Niño Southern Oscillation in a Changing Climate (eds McPhaden, M. J., Santoso, A. & Cai, W.) (AGU. 2020).
- 129. Chand, S. et al. Projected increase in El Niño-driven tropical cyclone frequency in the Pacific. Nat. Clim. Change 7, 123–127 (2017). Shows that, during future climate ENSO, tropical cyclones become more frequent during El Niño and less frequent during La Niña over the off-equatorial western Pacific and central North Pacific islands.
- 130. Ying, J., Huang, P., Lian, T. & Chen, D. Intermodel uncertainty in the change of ENSO's amplitude under global warming: role of the response of atmospheric circulation to SST anomalies. J. Clim. 32, 369–383 (2012)
- Rodríguez-Fonseca, B. et al. Are Atlantic Niños enhancing Pacific ENSO events in recent decades? Geophys. Res. Lett. 36, L20705 (2009).
- Ding, H., Keenlyside, N. S. & Latif, M. Impact of the equatorial Atlantic on the El Niño southern oscillation. *Clim. Dyn.* 38, 1965–1972 (2012).
- 133. Ham, Y.-G., Kug, J.-S., Park, J.-Y. & Jin, F.-F. Sea surface temperature in the north tropical Atlantic as a trigger for El Niño/Southern Oscillation events. *Nat. Geosci.* 6, 112–116 (2013).
- 134. Kug, J.-S. & Kang, I.-S. Interactive feedback between ENSO and the Indian Ocean. J. Clim. 19, 1784–1801 (2006).
- 135. Cai, W., Sullivan, A. & Cowan, T. Interactions of ENSO, the IOD, and the SAM in CMIP3 models. J. Clim. 24, 1688–1704 (2011).

- 136. Kucharski, F., Syed, F. S., Burhan, A., Farah, I. & Gohar, A. Tropical Atlantic influence on Pacific variability and mean state in the twentieth century in observations and CMIP5. Clim. Dyn. 44, 881–896 (2015).
- 137. Choi, J. Y., Ham, Y. G. & McGregor, S. Atlantic-Pacific SST gradient change responsible for the weakening of north tropical Atlantic-ENSO relationship due to global warming. *Geophys. Res. Lett.* 46, 7574–7582 (2019).
- 138. Jia, F., Wu, L., Gan, B. & Cai, W. Global warming attenuates the tropical Atlantic-Pacific teleconnection. *Sci. Rep.* **6**, 20078 (2016).
- 139. Jia, F. et al. Weakening Atlantic Niño—Pacific connection under greenhouse warming. Sci. Adv. 5, eaax4111 (2019).
- 140. Kug, J.-S., Vialard, J., Ham, Y.-G., Yu, J.-Y. & Lengaigne, M. ENSO remote forcing, in El Niño Southern Oscillation in a Changing Climate (eds McPhaden, M. J., Santoso, A. & Cai, W.) (AGU, 2020)
- Cheng, W., Chiang, J. C. H. & Zhang, D. Atlantic meridional overturning circulation (AMOC) in CMIP5 models: RCP and historical simulations. *J. Clim.* 26, 7187–7197 (2013).
- 142. Park, J. H. et al. Effect of recent Atlantic warming in strengthening Atlantic—Pacific teleconnection on interannual timescale via enhanced connection with the Pacific meridional mode. Clim. Dyn. 53, 371–387 (2019).
- 143. Wang, L., Yu, J.-Y. & Paek, H. Enhanced biennial variability in the Pacific due to Atlantic capacitor effect. *Nat. Commun.* **8**, 14887 (2017).
- 144. Le, T. & Bae, D.-H. Causal links on interannual timescale between ENSO and the IOD in CMIP5 future simulations. *Geophys. Res. Lett.* 46, 2820–2828 (2019).
 145. Sun, D.-Z. et al. Radiative and dynamical feedbacks
- 145. Sun, D.-Z. et al. Radiative and dynamical feedbacks over the equatorial cold tongue: results from nine atmospheric GCMs. J. Clim. 19, 4059–4074 (2006).
- 146. Lloyd, J., Guilyardi, E., Weller, H. & Slingo, J. The role of atmosphere feedbacks during ENSO in the CMIP3 models. Atmos. Sci. Lett. 10, 170–176 (2009).
- 147. Beobide-Arsuaga, G. et al. Uncertainty of ENSO-amplitude projections in CMIP5 and CMIP6 models. Clim. Dyn. 56, 3875–3888 (2021).
- 148. Guilyardi, E., Capotondi, A., Lengaigne, M., Thual, S. & Wittenberg, A. T. ENSO Modeling, in *El Niño Southern Oscillation in a Changing Climate* (eds McPhaden, M. J., Santoso, A. & Cai, W.) (AGU, 2020)
- 149. Bellenger, H., Guilyardi, E., Leloup, J., Lengaigne, M. & Vialard, J. ENSO representation in climate models: from CMIP3 to CMIP5. Clim. Dyn. 42, 1999–2018 (2014).
- Kim, S.-T., Cai, W., Jin, F.-F. & Yu, J.-Y. ENSO stability in coupled climate models and its association with mean state. Clim. Dyn. 42, 3313–3321 (2014).
 Bayr, T. et al. Error compensation of ENSO
- 151. Bayr, T. et al. Error compensation of ENSO atmospheric feedbacks in climate models and its influence on simulated ENSO dynamics. *Clim. Dyn.* 53, 155–172 (2019).
- 152. Watanabe, T. et al. Permanent El Niño during the Pliocene warm period not supported by coral evidence. *Nature* **471**, 209–211 (2011).
- 153. White, S. M. & Ravelo, A. C. Dampened El Niño in the early Pliocene warm period. *Geophys. Res. Lett.* 47, e2019GL085504 (2020).
 154. Fedorov, A. et al. The Pliocene paradox (mechanisms
- 154. Fedorov, A. et al. The Pliocene paradox (mechanisms for a permanent El Niño). *Science* 312, 1485–1489 (2006).
- Steph, S. et al. Early Pliocene increase in thermohaline overturning: A precondition for the development of the modern equatorial Pacific cold tongue. Paleoceanography 25, PA2202 (2010).
- 156. Manucharyan, G. E. & Fedorov, A. V. Robust ENSO across a wide range of climates. J. Clim. 27, 5836–5850 (2014).
- 157. Ford, H. L., Ravelo, A. C. & Polissar, P. J. Reduced El Niño–Southern oscillation during the last glacial maximum. *Science* 347, 255–258 (2015).
- Koutavas, A. & Joanides, S. El Niño—Southern oscillation extrema in the holocene and last glacial maximum. *Paleoceanography* 27, PA4208 (2012).
 Rustic, G. T., Koutavas, A., Marchitto, T. M. &
- 159. Rustic, G. T., Koutavas, A., Marchitto, T. M. & Linsley, B. K. Dynamical excitation of the tropical Pacific Ocean and ENSO variability by Little Ice Age cooling. Science 350, 1537–1541 (2015).
- 160. Sadekov, A. et al. Palaeoclimate reconstructions reveal a strong link between El Niño–Southern Oscillation and tropical Pacific mean state. *Nat. Commun.* 4, 2692 (2013).

- 161. Glaubke, R. H., Thirumalai, K., Schmidt, M. W. & Hertzberg, J. E. Discerning changes in high-frequency climate variability using geochemical populations of individual foraminifera. *Paleoceanogr. Paleoclimatol.* 36, e2020PA004065 (2021).
- 162. Wyman, D. A., Conroy, J. L. & Karamperidou, C. The tropical Pacific ENSO—mean state relationship in climate models over the last millennium. *J. Clim.* 33, 7539–7551 (2020).
- 163. Timmermann, A. & Jin, F. F. A nonlinear mechanism for decadal El Niño amplitude changes. *Geophys. Res. Lett.* 29, 1003 (2002).
- 164. Hayashi, M. & Jin, F. F. Subsurface nonlinear dynamical heating and ENSO asymmetry. *Geophys. Res. Lett.* 44, 12,427–12,435 (2017).
- 165. Conroy, J., Overpeck, J. T. & Cole, J. E. El Niño/ Southern Oscillation and changes in the zonal gradient of tropical Pacific sea surface temperature over the last 1.2 ka. *PAGES News* 18, 32–34 (2010)
- 166. Rustic, G. T., Polissar, P. J., Ravelo, A. C. & White, S. M. Modulation of late Pleistocene ENSO strength by the tropical Pacific thermocline. *Nat. Commun.* 11, 5377 (2020).
- 167. Liu, Z. Y. et al. Evolution and forcing mechanisms of El Niño over the past 21,000 years. *Nature* **515**, 550–553 (2014).
- 168. Karamperidou, C., Di Nezio, P. N., Timmermann, A., Jin, F.-F. & Cobb, K. M. The response of ENSO flavors to mid-Holocene climate: Implications for proxy interpretation. *Paleoceanography* 30, 527–547 (2015).
- 169. White, S. M., Ravelo, A. C. & Polissar, P. J. Dampened El Niño in the early and mid-Holocene due to insolationforced warming/deepening of the thermocline. *Geophys. Res. Lett.* 16, 316–326 (2018).
- Chen, L., Zheng, W. & Braconnot, P. Towards understanding the suppressed ENSO activity during mid-Holocene in PMIP2 and PMIP3 simulations. Clim. Dyn. 53, 1095

 –1110 (2019).
- Brown, J. R. et al. Comparison of past and future simulations of ENSO in CMIP5/PMIP3 and CMIP6/ PMIP4 models. Clim. Past. 16, 1777–1805 (2020)
- 172. Masson-Delmotte, V. et al. in Climate Change 2013: The Physical Science Basis. Contribution of Working Group I to the Fifth Assessment Report of the Intergovernmental Panel on Climate Change (eds Stocker, T. F. et al) 383–464 (Cambridge Univ. Press, 2013).
- 173. Tudhope, A. W. et al. Variability in the El Niño-Southern Oscillation through a glacial-interglacial cycle. *Science* 291, 1511–1517 (2001).
- 174. Rodbell, D. T. et al. An ~15,000-year record of El Niño-driven alluviation in southwestern Ecuador. *Science* **283**, 516–520 (1999).
- 175. Moy, C. M., Seltzer, G. O., Rodbell, D. T. & Anderson, D. M. Variability of El Niño/Southern Oscillation activity at millennial timescales during the Holocene epoch. *Nature* 420, 162–165 (2002).
- 176. Conroy, J. L., Overpeck, J. T., Cole, J. E., Shanahan, T. M. & Steinitz-Kannan, M. Holocene changes in eastern tropical Pacific climate inferred from a Galápagos lake sediment record. *Quat. Sci. Rev.* 27, 1166–1180 (2008).
- 177. Zhang, Z., Leduc, G. & Sachs, J. P. El Niño evolution during the Holocene revealed by a biomarker rain gauge in the Galápagos Islands. *Earth Planet. Sci. Lett.* 404, 420–434 (2014).
- 178. Chen, S. et al. A high-resolution speleothem record of western equatorial Pacific rainfall: Implications for Holocene ENSO evolution. *Earth Planet. Sci. Lett.* 442, 61–71 (2016).
- 179. Emile-Geay, J. Links between tropical Pacific seasonal, interannual and orbital variability during the Holocene. *Nat. Geosci.* 9, 168–173 (2016).
- 180. Carré, M. et al. Holocene history of ENSO variance and asymmetry in the eastern tropical Pacific. *Science* 345, 1045–1048 (2014).
- McGregor, S. et al. The effect of strong volcanic eruptions on ENSO, in El Niño Southern Oscillation in a Changing Climate (eds McPhaden, M. J., Santoso, A. & Cai, W.) (AGU, 2020).
- 182. Adams, J. B., Mann, M. E. & Ammann, C. M. Proxy evidence for an El Nino-like response to volcanic forcing. *Nature* 426, 274–278 (2003).
- 183. Emile-Geay, J., Seager, R., Cane, M. A., Cook, E. R. & Haug, G. H. Volcanoes and ENSO over the past millennium. J. Clim. 21, 3134–3148 (2008).
- 184. Ohba, M., Shiogama, H., Yokohata, T. & Watanabe, M. Impact of strong tropical volcanic eruptions on ENSO simulated in a coupled GCM. J. Clim. 26, 5169–5182 (2013).

- 185. Stevenson, S., Otto-Bliesner, B., Fasullo, J. & Brady, E. "El Niño like" hydroclimate responses to last millennium volcanic eruptions. *J. Clim.* 29, 2907–2921 (2016).
- 186. Khodri, M. et al. Tropical explosive volcanic eruptions can trigger El Nino by cooling tropical Africa. *Nat. Commun.* 8, 778 (2017).
- McGregor, S. & Timmermann, A. The effect of explosive tropical volcanism on ENSO. J. Clim. 24, 2178–2191 (2011).
- 188. Zanchettin, D. et al. Bidecadal variability excited in the coupled ocean—atmosphere system by strong tropical volcanic eruptions. Clim. Dyn. 39, 419–444 (2012)
- 189. Robock, A. Volcanic eruptions and climate. *Rev. Geophys.* **38**, 191–219 (2000).
- 190. Ding, Y. et al. Ocean response to volcanic eruptions in Coupled Model Intercomparison Project 5 (CMIP5) simulations. *J. Geophys. Res. Oceans* 119, 5622–5637 (2014).
- Dee, S. G. et al. No consistent ENSO response to volcanic forcing over the last millennium. *Science* 367, 1477–1481 (2020).
 - Shows that proxy records reveal an insignificant tendency for an El Nino-like response in the year after a strong volcanic eruption, at odds with the strong tendencies found in climate models.
- 192. Pausata, F. S. R., Karamperidou, C., Caballero, R. & Battisti, D. S. ENSO response to high-latitude volcanic eruptions in the Northern Hemisphere: The role of the initial conditions. *Geophys. Res. Lett.* 43, 8694–8702 (2016).
- Stevenson, S., Fasullo, J. T., Otto-Bliesner, B. L., Tomas, R. A. & Gao, C. Role of eruption season in reconciling model and proxy responses to tropical volcanism. *Proc. Natl Acad. Sci. USA* 114, 1822–1826 (2017).
- 194. Zanchettin, D. et al. Clarifying the relative role of forcing uncertainties and initial-condition unknowns in spreading the climate response to volcanic eruptions. *Geophys. Res. Lett.* 46, 1602–1611 (2019).
- 195. Pausata, F. S. R., Zanchettin, D., Karamperidou, C., Caballero, R. & Battisti, D. S. ITCZ shift and extratropical teleconnections drive ENSO response to volcanic eruptions. Sci. Adv. 6, eaaz5006 (2020).
- 196. Predybaylo, E. et al. El Niño/Southern Oscillation response to low-latitude volcanic eruptions depends on ocean pre-conditions and eruption timing. Commun. Farth Environ. 1, 12 (2020).
- 197. Emile-Geay, J. & Tingley, M. Inferring climate variability from nonlinear proxies: application to palaeo-ENSO studies. *Clim. Past.* 12, 31–50 (2016). Demonstrates the pitfalls of ignoring nonlinearities in the proxy-climate relationship, which often exaggerates climate variability changes inferred by proxies and leads to reconstructions with poorly quantified uncertainties.
- 198. Kiefer, J. & Karamperidou, C. High-resolution modeling of ENSO-induced precipitation in the tropical Andes: Implications for proxy interpretation. *Paleoceanogr. Paleoclimatol.* 34, 217–236 (2019).
- 199. Dee, S., Okumura, Y., Stevenson, S. & Di Nezio, P. Enhanced North American ENSO teleconnections during the Little Ice Age revealed by paleoclimate data assimilation. *Geophys. Res. Lett.* 47, e2020GL087504 (2020).
- 200. Chang, P. et al. Pacific meridional mode and El Niño — Southern Oscillation. *Geophys. Res. Lett.* 34, L16608 (2007).
- Vimont, D. J., Alexander, M. & Fontaine, A. Midlatitude excitation of tropical variability in the Pacific: The role of thermodynamic coupling and seasonality. J. Clim. 22, 518–534 (2009).
- 202. Stuecker, M. F. Revisiting the Pacific meridional mode. *Sci. Rep.* **8**, 3216 (2018).
- Hong, L. C. & Jin, F. F. A southern hemisphere booster of super El Niño. *Geophys. Res. Lett.* 41, 2142–2149 (2014).
- Holmes, R. M., McGregor, S., Santoso, A. & England, M. H. Contribution of tropical instability waves to ENSO irregularity. *Clim. Dyn.* 52, 1857–1855 (2019).
- Bony, S. & Dufresne, J. L. Marine boundary layer clouds at the heart of tropical cloud feedback uncertainties in climate models. *Geophys. Res. Lett.* 32, L20806 (2005).
- Deser, C. et al. Insights from Earth system model initial-condition large ensembles and future prospects. Nat. Clim. Change 10, 277–286 (2020).
- 207. Hawkins, E. & Sutton, R. Time of emergence of climate signals. *Geophys. Res. Lett.* **39**, L01702 (2012).

- Jochum, M. & Murtugudde, R. Temperature advection by tropical instability waves. *J. Phys. Oceanogr.* 36, 592–605 (2006).
- 209. An, S. I. Interannual variations of the tropical ocean instability wave and ENSO. *J. Clim.* **21**, 3680–3686 (2008)
- Bartlein, P. J. & Shafer, S. L. Paleo calendar-effect adjustments in time-slice and transient climate-model simulations (PaleoCalAdjust v1.0): impact and strategies for data analysis. *Geosci. Model. Dev.* 12, 3889–3913 (2019).

Acknowledgements

This work is supported by the Strategic Priority Research Program of the Chinese Academy of Sciences, grant no. XDB40000000. W.C., A.S., B.N. and G.W. are supported by the Centre for Southern Hemisphere Oceans Research (CSHOR), a joint research facility between Qingdao National Laboratory for Marine Science and Technology (QNLM) and Commonwealth Scientific and Industrial Research Organisation (CSIRO), and the Earth System and Climate Change Hub of the Australian Government's National Environment Science Program. M.F.S. was supported by the NOAA's Climate Program Office's Modeling, Analysis, Predictions, and Projections (MAPP) Program grant NA20OAR4310445 and participates in the MAPP Marine Ecosystem Task Force. This is Pacific Marine Environmental Laboratory (PMEL) contribution number 5213. M.L. is supported by the ARISE ANR (Agence Nationale pour la Recherche) project (ANR-18-CE01-0012). X. Lin is supported by the National Natural Science Foundation of China (41925025 and 92058203). B.G. was supported by the National Natural Science Foundation of China (41922039). A.C. is supported by the NOAA's Climate Program Office Climate Variability and Predictability (CVP) and MAPP programs. M.C. was supported by NERC grant NE/S004645/1. This is IPRC publication 1525 and SOEST contribution 11356. A.S.T. is supported by the Australian Research Council (ARC FT160100495), S.-W.Y. is funded by the Korean Meteorological Administration Research and Development Program under grant (KMI2020-01213). Y.Y. is supported by the National Natural Science Foundation of China (NSFC) proiect (grant no. 41976005), X. Li is supported by National Key R&D Program of China (2018YFA0605703) and the National Natural Science Foundation of China (grant 41976193). M.C. is supported by NERC grant NE/S004645/1. T.B. is funded by Deutsche Forschungsgemeinschaft (DFG) project "Influence of Model Bias on ENSO Projections of the 21st Century" through grant 429334714. C.K. is supported by US NSF award AGS-1902970. J.R.B. acknowledges support from the ARC Centre of Excellence for Climate Extremes (CE170100023). J.Y. is supported by the National Natural Science Foundation of China (grants 41690121 and 41690120). A.T. was supported by the Institute for Basic Science (IBS-R028-D1). S.M. acknowledges support from the Australian Research Council through grant number Ft160100162. J.-S.K. is supported by the National Research Foundation of Korea (NRF 2018R1A5A1024958). X.-T.Z. is funded by the National Natural Science Foundation of China (41975092), B.D. acknowledges support from Fondecyt (grant 1190276) and ANR (grant ANR-18-CE01-0012). We acknowledge the World Climate Research Programme, which, through its Working Group on Coupled Modelling, coordinated and promoted CMIP6. We thank the climate modelling groups for producing and making available their model output, the Earth System Grid Federation (ESGF) for archiving the data and providing access, and the multiple funding agencies who support CMIP6 and ESGF. PMIP is endorsed by both WCRP/WGCM and Future Earth/PAGES.

Author contributions

W.C. and A.S. conceived the study. W.C., M.J.M., M.F.S., M.L., A.S., J-S.K., A.S.T., S.-W.Y., C.K., B.D., M.C. and A.T. coordinated the presentation and discussion for various sections. F.J., B.N., G.W., Y.Y. and J.Y. contributed to analysis and the graphics of various figures. All authors contributed to the manuscript preparation, interpretation, discussion and writing, led by W.C.

Competing interests

The authors declare no competing interests.

Peer review information

Nature Reviews Earth & Environment thanks Nathaniel Johnson and the other, anonymous, reviewer(s) for their contribution to the peer review of this work.

Publisher's note

Springer Nature remains neutral with regard to jurisdictional claims in published maps and institutional affiliations.

© Springer Nature Limited 2021